Fig. 4

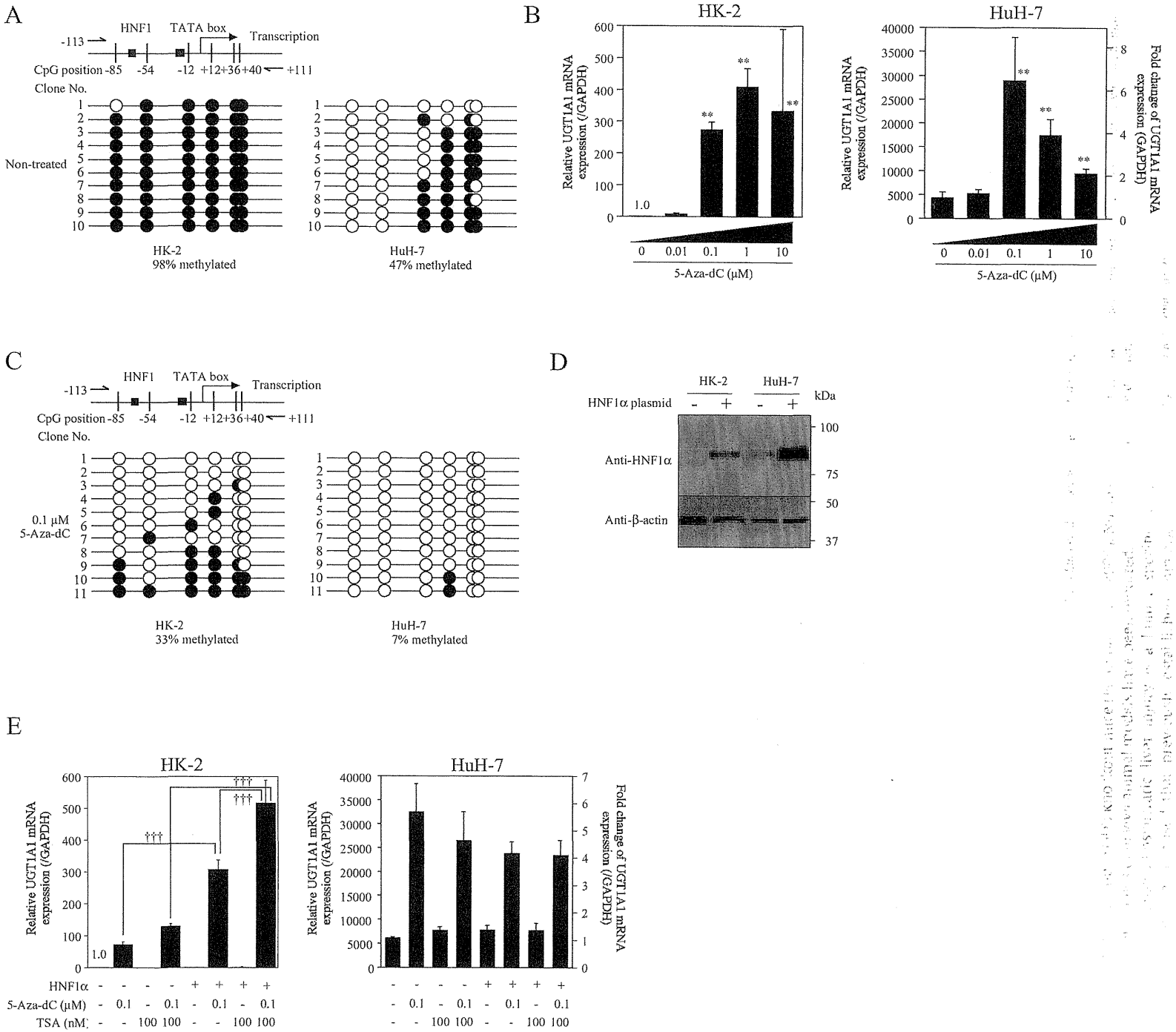
A
HNF1
TATA box
Transcription
-113
CpG position -85 -54 -12 +12+36+40 +111
Clone No.
Non-treated
HK-2
98% methylated
HuH-7
47% methylated
B
HK-2
HuH-7
Relative UGT1A1 mRNA expression (/GAPDH)
Fold change of UGT1A1 mRNA expression (GAPDH)
1.0
0 0.01 0.1 1 10
5-Aza-dC (μM)
C
0.1 μM 5-Aza-dC
HK-2
33% methylated
HuH-7
7% methylated
D
HK-2
HuH-7
HNF1α plasmid
kDa
Anti-HNF1α
Anti-β-actin
100
75
50
37
E
HK-2
HuH-7
HNF1α
5-Aza-dC (μM)
TSA (nM)

Toxicology Letters 214 (2012) 9–18

Contents lists available at SciVerse ScienceDirect

Toxicology Letters

journal homepage: www.elsevier.com/locate/toxlet

Chimeric mice with a humanized liver as an animal model of troglitazone-induced liver injury

Masakazu Kakuni[a], Mayu Morita[b], Kentaro Matsuo[b], Yumiko Katoh[a], Miki Nakajima[b], Chise Tateno[a], Tsuyoshi Yokoi[b,*]

[a] PhoenixBio Co., Ltd., Hiroshima 739-0046, Japan
[b] Division of Pharmaceutical Sciences, Faculty of Pharmaceutical Sciences, Kanazawa University, Kakuma-machi, Kanazawa 920-1192, Japan

HIGHLIGHTS

- Troglitazone (Tro) was withdrawn due to its association with severe liver injury.
- Orally administered Tro has never induced liver injury in experimental animals.
- The chimeric mice with a humanized liver reproduced Tro-induced liver injury.
- Possible factors that contribute to the Tro-induced liver injury were evaluated.
- This mouse model enables human hepatocytes to be examined in an *in vivo* environment.

ARTICLE INFO

Article history:
Received 11 April 2012
Received in revised form 31 July 2012
Accepted 2 August 2012
Available online xxx

Keywords:
Chimeric mouse with a humanized liver
Drug-induced liver injury (DILI)
Hepatotoxicity
Troglitazone
Glutathione

ABSTRACT

Troglitazone (Tro) is a thiazolidinedione antidiabetic drug that was withdrawn from the market due to its association with idiosyncratic severe liver injury. Tro has never induced liver injury in experimental animals *in vivo*. It was assumed that the species differences between human and experimental animals in the pharmaco- or toxicokinetics of Tro might be associated with these observations. In this study, we investigated whether a chimeric mouse with a humanized liver that we previously established, whose replacement index with human hepatocytes is up to 92% can reproduce Tro-induced liver injury. When the chimeric mice were orally administered Tro for 14 or 23 days (1000 mg/kg/day), serum alanine aminotransferase (ALT) was significantly increased by 2.1- and 3.6-fold, respectively. Co-administration of L-buthionine sulfoximine (10 mM in drinking water), an inhibitor of glutathione (GSH) synthesis, unexpectedly prevented the Tro-dependent increase of ALT, which suggests that the GSH scavenging pathway will not be involved in Tro-induced liver injury. To elucidate the mechanism of the onset of liver injury, hepatic GSH content, the level of oxidative stress markers and phase I and phase II drug metabolizing enzymes were determined. However, these factors were not associated with Tro-induced liver injury. An immune-mediated reaction may be associated with Tro-induced liver toxicity *in vivo*, because the chimeric mouse is derived from an immunodeficient SCID mouse. In conclusion, we successfully reproduced Tro-induced liver injury using chimeric mice with a humanized liver, which provides a new animal model for studying idiosyncratic drug-induced liver injury.

1. Introduction

Troglitazone (Tro) was the first thiazolidinedione used for treating of type II diabetes mellitus, but was withdrawn due to serious idiosyncratic liver injury. During the preclinical development of Tro, no study could predict the hepatotoxic effect of Tro in human (Watanabe et al., 1999). After the withdrawal of Tro from the market, numerous studies using animal models were performed to reproduce the hepatotoxicity of Tro, but almost all were unsuccessful (Bedoucha et al., 2001; Jia et al., 2000; Watanabe et al., 2000).

Ong et al. (2007) reported that the administration of Tro (30 mg/kg, *i.p.*) to heterozygous superoxide dismutase 2 (SOD2) knockout (*SOD2*$^{+/-}$) mice resulted in hepatocellular necrosis and increased serum alanine aminotransferase (ALT) levels, suggesting that SOD2, which is expressed mainly in the mitochondria, plays a crucial role in Tro-induced liver injury. However, other research group could not reproduce these results using the same

* Corresponding author at: Drug Metabolism and Toxicology, Faculty of Pharmaceutical Sciences, Kanazawa University, Kakuma-machi, Kanazawa 920-1192, Japan. Tel.: +81 76 234 4407; fax: +81 76 234 4407.
E-mail address: tyokoi@kenroku.kanazawa-u.ac.jp (T. Yokoi).

0378-4274/$ – see front matter © 2012 Elsevier Ireland Ltd. All rights reserved.
http://dx.doi.org/10.1016/j.toxlet.2012.08.001

heterozygous SOD2 knockout mice (Fujimoto et al., 2009). No further studies of *in vivo* animal models have been reported.

Because idiosyncratic liver injury is a human-specific toxic event, we surmised that previously established chimeric mice with a humanized liver (Tateno et al., 2004) might be useful as an animal model. In this study, we investigated whether Tro causes liver injury in a chimeric mouse with a humanized liver, which was derived from a urokinase-type plasminogen activator$^{+/+}$/severe combined immunodeficient transgenic (uPA$^{+/+}$/SCID mouse) mouse line. In this animal model, more than 75% of the mouse hepatocytes are replaced with human hepatocytes in which the human mRNAs and proteins expression levels and enzyme activities were evaluated (Katoh et al., 2004, 2005, 2007; Nishimura et al., 2005).

Tro undergoes metabolic activation by CYPs, in particular, the CYP3A4 isoform, to form reactive metabolites that bind covalently to proteins and nucleophiles, such as glutathione (GSH) and cysteine. Various reactive metabolites of Tro were identified as GSH conjugates (Tettey et al., 2001; Kassahun et al., 2001; He et al., 2004). The susceptibility of drugs metabolized to reactive intermediates is different between GSH-depleted animals and normal animals (T. Watanabe et al., 2003; Usui et al., 2011). Therefore, we expected that Tro would exhibit hepatotoxic effects under a GSH-depleted condition. L-Buthionine sulfoximine (BSO), a well-known inhibitor of GSH synthesis, was selected to investigate the relationship between the GSH conjugation ability and Tro-induced hepatotoxicity.

In the present study, we orally administered Tro for 14 or 23 days to chimeric mice with a humanized liver and reproduced liver injury. Subsequently, possible factors that were expected to contribute to the development of Tro-induced liver injury, such as drug-metabolizing enzymes, GSH, SOD2, and protein carbonyl contents, were evaluated.

2. Materials and methods

2.1. Chemicals

TRO was kindly provided by Daiichi Sankyo (Tokyo, Japan). L-Buthionine sulfoximine (BSO) and paclitaxel were purchased from Sigma (St. Louis, MO). ReverTra Ace was from Toyobo (Tokyo, Japan). Random hexamer, RNAiso, SYBR Premix Ex Taq, and ROX Reference Dye II were from Takara (Osaka, Japan). Recombinant human CYP2C8 and CYP3A4 expressed in baculovirus-infected insect cells and 6a-hydroxypaclitaxel were from BD Gentest (Woburn, MA). Dexamethasone and testosterone were from Wako Pure Chemical Industries (Osaka, Japan). 6b-Hydroxytestosterone was from Sekisui Medical (Tokyo, Japan). All primers were commercially synthesized at Hokkaido System Sciences (Sapporo, Japan). The polyclonal rabbit anti-human CYP2C8 antibody was from Nosan (Yokohama, Japan) and the polyclonal goat anti-CYP3A antibody (sc-30621) was from Santa Cruz Biotechnology (Santa Cruz, CA). All other chemicals were of analytical or the highest grade commercially available.

2.2. Generation of the chimeric mice with a humanized liver

The present study was conducted in accordance with the National Institutes of Health Guide for Animal Welfare of Japan, and the protocols were approved by the Institutional Animal Care and Use Committees of Kanazawa University (Kanazawa, Japan) and PhoenixBio Co., Ltd. (Hiroshima, Japan). The chimeric mice were generated by PhoenixBio. Briefly, commercially available cryopreserved human hepatocytes (5-year-old African-American male from BD Gentest) were transplanted into the spleens of uPA$^{+/+}$/SCID mice at approximately 3–4 weeks of age. At mice's age of 6–7 weeks, the monitoring of human albumin (h-Alb) concentration in blood was started and continued until the start of the study when the chimeric mice were 11–15 weeks old. Two microliters of blood was collected from tail vein of the mice once per week, and the concentrations of hAlb in the blood of the chimeric mice were determined by latex agglutination immunonephelometry to estimate the rate of replacement of mouse hepatocytes with human hepatocytes (RI: Replacement Index). The correlation between hAlb and the actual RI has been determined based on immunohistochemistry conducted with anti-human specific cytokeratin 8 and 18 antibodies (Tateno et al., 2004). The chimeric mice used in the present study were female, 11–15 weeks old, and exhibited concentrations of 8.0–14.9 mg/ml of hAlb or an RI of 75–92% at the start of the TRO administration (Table 1). The animals were housed in a controlled environment (temperature 23 ± 1 °C, humidity 57 ± 15%, and 12 h light/12 h dark cycle) in the institution's animal facility with *ad libitum* access to food and water.

2.3. Drug and/or BSO administration

The chimeric mice were orally administered Tro [250 mg/kg/10 ml, 500 mg/kg/ml or 1000 mg/kg/10 ml, suspended in 0.5% carboxymethylcellulose (CMC)] once daily for 14 (1000 mg/kg), 23 (1000 mg/kg) or 28 (250 and 500 mg/kg) days in a non-fasting condition, and 0.5% CMC was administered once daily as a control. BSO (10 mM) in sterilized tap water was also administered *via* drinking water alone or with Tro. Water bottle was changed twice a week during the BSO treatment. The dosing method was originally reported by T. Watanabe et al. (2003), in which 5–30 mM of BSO in drinking water had been confirmed to be stable for 15 days at 23 °C without light-shielded conditions. Pre-dosing blood samples were collected under isoflurane anesthesia to measure the initial serum ALT level. Twenty-four hours after the last Tro administration, the blood and livers were collected by exsanguination under isoflurane anesthesia. Serum ALT, aspartate aminotransferase (AST), bilirubin (total bilirubin: T-Bil, and direct bilirubin: D-Bil) and lactate dehydrogenase (LDH) levels were measured using FUJI DRI-CHEM (FUJIFILM, Tokyo, Japan). A portion of the liver was fixed in buffered neutral 10% formalin. The fixed samples were embedded in paraffin, sectioned at a thickness of 2 μm and stained with hematoxylin–eosin (H&E) for microscopic examination.

2.4. GSH level

Mouse livers were homogenized in ice-cold 5% sulfosalicylic acid using a glass homogenizer and centrifuged at 8000 × *g* at 4 °C for 10 min. The GSH concentration in the supernatant was measured as described previously (Tietze, 1969).

2.5. Glutathione S-transferase (GST) activity

GST activity was measured according to the method of Habig et al. (1974) with slight modifications. The incubation mixtures consisted of cytosol (0.1 ml) in 125 mM potassium phosphate buffer (pH 6.5) containing 1.25 mM GSH (0.8 ml) and 10 mM 1-chloro-2,4-dinitrobenzene in 40% ethanol (0.1 ml). The reaction mixture was incubated at 25 °C for 10 min and monitored at 340 nm.

2.6. SOD2 activity

SOD2 activity was measured using a Superoxide Dismutase Assay kit (Cayman Chemical, Ann Arbor, MI). The method utilizes tetrazolium salt to quantify the superoxide radicals generated by xanthine oxidase and hypoxanthine. The standard curve was generated using a quality controlled SOD standard in the kit. SOD2 activity was determined in the presence of potassium cyanide to inhibit SOD1 activity.

2.7. Protein carbonyl content

Plasma protein carbonyl content was measured using an OxiSelect Protein Carbonyl ELISA kit (Cell Biolabs, Tokyo, Japan) as described previously (Yoshikawa et al., 2009).

2.8. Real-time reverse transcription (RT)-PCR

Total hepatic RNA was isolated using RNAiso according to the manufacturer's instructions. Human CYP2C8, CYP3A4, SULT1A1, UGT1A1 and GAPDH mRNA levels were quantified by real-time RT-PCR. Total RNA (4 μg) and 150 ng random hexamer were mixed and incubated at 70 °C for 10 min. An RNA solution was added to a reaction mixture that contained 100 units of ReverTra Ace, reaction buffer and 0.5 mM dNTPs in a final volume of 40 μl. The reaction mixture was incubated at 30 °C for 10 min, 42 °C for 1 h, and then heated at 98 °C for 10 min to inactivate the enzyme. Real-time RT-PCR was performed using the Mx3000P (Stratagene, La Jolla, CA). The PCR mixture contained 1 μl of template cDNA, SYBR Premix Ex Taq solution, and 10 pmol of sense and antisense primers. The human-specific primer sequences used in this study are shown in Table 2. The amplified products were monitored directly by measuring the intensity of the SYBR Green I dye (Molecular Probes, Eugene, OR) that binds to the PCR amplified double-stranded DNA.

2.9. Immunoblot analysis

SDS-polyacrylamide gel electrophoresis and immunoblot analysis of human CYP2C8 and CYP3A were performed according to Katoh et al. (2004). The liver microsomes (2 or 20 μg) were separated on 10% polyacrylamide gel and transferred electrophoretically to a polyvinylidene difluoride membrane. Recombinant human P450s were applied as standards. Biotinylated anti-rabbit or goat IgG and a Vectastain ABC kit (Vector Laboratories, Burlingame, CA) were used for diaminobenzidine staining. It was confirmed that the human P450 antibodies in this experimental condition did not cross-react with the mouse orthologs.

Table 1
Chimeric mice used in this study.

Group	Mouse no.	Age at 1st dose (week)	hAlb concentration in the blood (mg/ml)	Approximate RI (%)
Control	1	13	9.6	80
	2	13	11.6	85
	3	13	9.1	78
	4	11	8.0	75
	5	12	9.3	79
	6	12	11.6	85
Tro 1000 mg/kg (14 days)	7	13	11.7	85
	8	13	9.6	80
	9	13	9.1	78
	10	14	9.7	80
	11	13	9.6	80
Tro 250 mg/kg (28 days)	S1	12	9.3	79
	S2	12	8.4	76
	S3	12	10.5	82
	S4	12	9.0	78
	S5	12	10.6	83
Tro 500 mg/kg (28 days)	S6	12	9.7	80
	S7	12	9.6	80
	S8	11	9.1	78
	S9	12	8.2	75
	S10	15	9.5	80
Tro 1000 mg/kg (23 days)	12	15	14.9	92
	13	14	12.3	87
	14	14	14.6	92
	15	15	8.3	76
BSO (14 days)	16	13	10.3	82
	17	13	9.2	79
	18	13	11.6	85
BSO + Tro 1000 mg/kg (14 days)	19	13	8.7	77
	20	13	10.3	82
	21	13	9.2	79

RI, replacement index.

Table 2
Sequence of primers for real-time RT-PCR analyses.

Primer	Sequence
CYP2C8 S[a]	5′-AGATCAGAATTTCTCACCC-3′
CYP2C8 AS[a]	5′-AACTTCGTGTAAGAGCAACA-3′
CYP3A4 S[a]	5′-CCAAGCTATGCTCTTCACCG-3′
CYP3A4 AS[a]	5′-TCAGGTCCACTTACGGTGC-3′
SULT1A1 S	5′-ATGGAGACTCTGAAAGACACACCGG-3′
SULT1A1 AS	5′-TGTGCTGAACCACGAAGTCCACG-3′
UGT1A1 S[b]	5′-CCTTGCCTCAGAATTCCTTC-3′
UGT1A1 AS[b]	5′-ATTGATCCCAAAGAGAAAACCAC-3′
GAPDH S[a]	5′-CCAGGGCTTTTAACTC-3′
GAPDH AS[a]	5′-GCTCCCCCCTGCAAATGA-3′

S, sense primer; AS, antisense primer.
[a] From Katoh et al. (2004).
[b] From Izukawa et al. (2009).

2.10. CYP2C8 and CYP3A4 activities

Liver microsomes from the chimeric or control mice were prepared as described previously (Katoh et al., 2004) and stored at −80 °C until analysis. The protein concentration was determined using Bradford assay reagent (Bio-Rad, Hercules, CA) with bovine γ globulin as the standard. The typical incubation mixtures (total volume, 0.2 ml) consisted of microsomes in 100 mM potassium phosphate buffer (pH 7.4) containing an NADPH-generating system (0.5 mM $NADP^+$, 5 mM glucose 6-phosphate, 5 mM $MgCl_2$, and 1 unit/ml glucose-6-phosphate dehydrogenase) and a substrate.

Paclitaxel 6α-hydroxylase activity was determined by the method of Willey et al. (1993), with slight modifications. The concentrations of the microsomes and paclitaxel were 0.5 mg/ml and 20 μM, respectively. The reaction mixture was incubated at 37 °C for 10 min, and terminated by adding 1.0 ml of dichloromethane. Testosterone (10 μl of 100 μM) was added as an internal standard. After centrifugation at 900 × *g* for 10 min, the organic phase (500 μl) was evaporated under a gentle stream of nitrogen at 40 °C. The residue was redissolved in 200 μl of mobile phase and then 100-μl portion of the sample was subjected to high-performance liquid chromatography (HPLC). The product formation was determined with a Mightysil RP-8 C8 GP column (5-μm particle size, 4.6 i.d. × 150 mm; Kanto Chemical, Tokyo, Japan). The mobile phase (45% acetonitrile/20 mM ammonium acetate) was used under isocratic condition. The flow rate was 1.0 ml/min, and the column temperature was 35 °C. The eluent was monitored at 227 nm. The quantification of 6α-hydroxypaclitaxel was performed by comparing the HPLC peak heights to that of authentic standards with reference to an internal standard. The retention time of 6α-hydroxypaclitaxel and paclitaxel was 9.0 and 14.7 min, respectively.

The dexamethasone 6-hydroxylase activity was determined according to the method of Tomlinson et al. (1997), with slight modifications. The concentrations of microsomes and dexamethasone were 1.0 mg/ml and 100 μM, respectively. The reaction mixture (total volume, 0.2 ml) was incubated at 37 °C for 30 min, and terminated by adding 1.5 ml of ice-cold ethyl acetate. 6-Hydroxytestosterone (10 μl of 10 ng/μl) was added as an internal standard. After centrifugation at 900 × *g* for 10 min, the organic phase (500 μl) was evaporated under a gentle stream of nitrogen at 40 °C. The residue was redissolved in 200 μl of mobile phase and then 100-μl portion of the sample was subjected to HPLC. The product formation was determined with a Mightysil RP-8 C8 GP column (5-μm particle size, 4.6 i.d. × 150 mm; Kanto Chemical). The mobile phase (23% acetonitrile/0.015% formic acid) was used under isocratic condition. The flow rate was 1.0 ml/min, and the column temperature was 35 °C. The eluent was monitored at 243 nm. The dexamethasone 6-hydroxylase activity was quantified using a standard curve of dexamethasone because we could not obtain pure 6-hydroxydexamethasone. The retention time of 6-hydroxydexamethasone was confirmed using the incubation product of recombinant CYP3A4 and dexamethasone. The retention time of 6-hydroxydexamethasone and dexamethasone was 4.8 and 37.7 min respectively. The final concentration of the solvent in the incubation mixture was less than 1%.

2.11. Statistical analysis

Statistical analyses between multiple groups were performed using one-way analysis of variance (ANOVA), followed by Dunnett's *post hoc* test. Comparisons between two groups were performed using two-tailed Student's *t*-test. A value of $P < 0.05$ was considered statistically significant.

Table 3
Serum biochemical parameters in toroglitazone and/or BSO-administered chimeric mice.

Group	Mouse no.	ALT (U/l)			AST (U/l)		LDH (U/l)		T-Bil (mg/dl)		D-Bil (mg/dl)	
		Initial	Final		Final		Final		Final		Final	
Control	1	108	77		147		1366		0.8		0.1	
	2	90	56		83		2884		0.7		0.1	
	3	140	139		212		1386		0.8		0.1	
	4	87	137		152		1554		0.8		ND	
	5	88	79		126		832		0.9		ND	
	6	92	106		188		1122		0.8		ND	
	Mean ± SD	101 ± 21	99 ± 34	[1.0]	151 ± 46	[1.0]	1524 ± 712	[1.0]	0.8 ± 0.1	[1.0]	0.1 ± 0.0	[1.0]
Tro 1000 mg/kg (14 days)	7	64	67		170		3600		0.9		0.1	
	8	96	233	R	345		2520		1.5		0.4	
	9	144	218	R	283		861		1.0		0.1	
	10	79	167	R	188		1724		0.8		0.1	
	11	39	64		145		897		0.9		0.1	
	Mean ± SD	84 ± 39	150 ± 81	[1.5]	226 ± 84	[1.5]	1920 ± 1161	[1.3]	1.0 ± 0.3	[1.3]	0.2 ± 0.1	[2.0]
	R (n = 3)	106 ± 34	206 ± 35**	[2.1]	272 ± 79	[1.8]	1702 ± 830	[1.1]	1.1 ± 0.4	[1.4]	0.2 ± 0.2	[2.0]
Tro 250 mg/kg (28 days)	S1	62	344	R	361		2256		0.9		ND	
	S2	71	182		250		902		0.9		ND	
	S3	75	70		165		1498		0.7		ND	
	S4	59	146	R	186		823		0.8		ND	
	S5	80	111		130		667		0.8		ND	
	Mean ± SD	69 ± 9	171 ± 105	[1.7]	218 ± 91	[1.4]	1229 ± 655	[0.8]	0.8 ± ± 0.1	[1.0]	0.1 ± 0.0	[1.0]
Tro 500 mg/kg (28 days)	S6	66	108		144		779		0.7		ND	
	S7	78	205	R	318		1126		0.7		ND	
	S8	79	48		93		531		0.6		ND	
	S9	81	91		114		487		0.7		ND	
	S10	71	171	R	170		982		0.6		ND	
	Mean ± SD	75 ± 6	125 ± 63	[1.3]	168 ± 89	[1.1]	781 ± 278	[0.5]	0.7 ± 0.1	[0.9]	0.1 ± 0.0	[1.0]
Tro 1000 mg/kg (23 days)	12	79	504	R	452		1566		0.6		0.1	
	13	70	221	R	260		1550		0.7		0.1	
	14	84	345	R	410		1274		0.7		0.1	
	15	113	97		138		729		0.7		ND	
	Mean ± SD	87 ± 19	292 ± 174	[2.9]	315 ± 144	[2.1]	1280 ± 391	[0.8]	0.7 ± 0.1	[0.9]	0.1 ± 0.0	[1.0]
	R (n = 3)	78 ± 7	357 ± 142**	[3.6]	374 ± 101**	[2.5]	1463 ± 164	[1.0]	0.7 ± 0.1	[0.9]	0.1 ± 0.0	[1.0]
BSO (14 days)	16	58	51		102		1728		0.8		0.2	
	17	65	91		131		1206		0.6		0.1	
	18	53	38		123		1504		0.7		0.1	
	Mean ± SD	59 ± 6	60 ± 28	[0.6]	119 ± 15	[0.8]	1479 ± 262	[1.0]	0.7 ± 0.1	[0.9]	0.1 ± 0.1	[1.0]
BSO + Tro 1000 mg/kg (14 days)	19	117	59		175		1572		0.7		0.2	
	20	55	55		105		891		0.6		ND	
	21	76	39		144		836		0.8		0.1	
	Mean ± SD	83 ± 32	51 ± 11	[0.5]	141 ± 35	[0.9]	1100 ± 410	[0.7]	0.7 ± 0.1	[0.9]	0.2 ± 0.1	[2.0]

Each parameter except initial value was measured 24 h after the last troglitazone administration.
Differences compared to the control group were considered significant at $^{**}P < 0.01$.
ND, not detected; R, responder; score in parenthesis, ratio to the control.

3. Results

3.1. TRO caused liver injury in chimeric mice with a humanized liver

TRO was orally administered to female chimeric mice at a dose of 250 mg/kg/day for 28 days (Tro 250-28 day), 500 mg/kg/day for 28 days (Tro 500-28 day), and 1000 mg/kg/day for 14 days (Tro 1000-14 day) or 23 days (Tro 1000-23 day) in a non-fasting condition. BSO (10 mM in drinking water) was treated alone or with Tro administration for 14 days. The initial serum ALT levels ranged from 39 to 144 U/l among all animals (Table 3). The final ALT levels in the Tro 250-28 day (171 ± 105 U/l), Tro 500-28 day (125 ± 63 U/l), Tro 1000-14 day (150 ± 81 U/l) and Tro 1000-23 day (292 ± 174 U/l) groups increased by 1.7-, 1.3-, 1.5- and 2.9-fold, respectively compared to the control group (99 ± 34 U/l). Two out of five mice in both Tro 250-28 day and Tro 500-28 day groups, three out of five mice in the Tro 1000-14 day group and three out of four mice in the Tro 1000-23 day group showed increased ALT levels of more than 144 U/l, the highest initial ALT level among all mice. These mice were termed responders (R) in Table 3. The average values of ALT levels in Tro 250-28 day and Tro 500-28 day groups are a little higher than the control group, however there is no clear dose–response in these values. These results suggest that the dose level of 1000 mg/kg is required for the onset of troglitazone-induced liver injury in the chimeric mice. Therefore, we put focus on the results from 1000 mg/kg dose groups in the subsequent analyses. The final ALT levels in responders in the Tro 1000-14 day and Tro 1000-23 day groups were significantly higher than those in the control group by 2.1- and 3.6-fold, respectively (Fig. 1). For the subsequent analyses, the data from the responders (R) in Tro 1000-14 day and Tro 1000-23 day groups were compared to those in the control group.

The final AST level in the Tro 1000-23 day group was significantly higher than that in the control group by 2.5-fold. The final serum LDH, T-Bil and D-Bil levels in the Tro 1000-14 day and Tro 1000-23 day groups were unchanged compared to the control group (Table 3). The LDH, T-Bil and D-Bil levels in the Tro 1000-23 day group were lower than those in the Tro 1000-14 day group. Both in the BSO alone and BSO- and Tro-administered groups, serum ALT, AST, LDH, T-Bil and D-Bil levels were unchanged compared to the levels in the control group (Table 3 and Fig. 1).

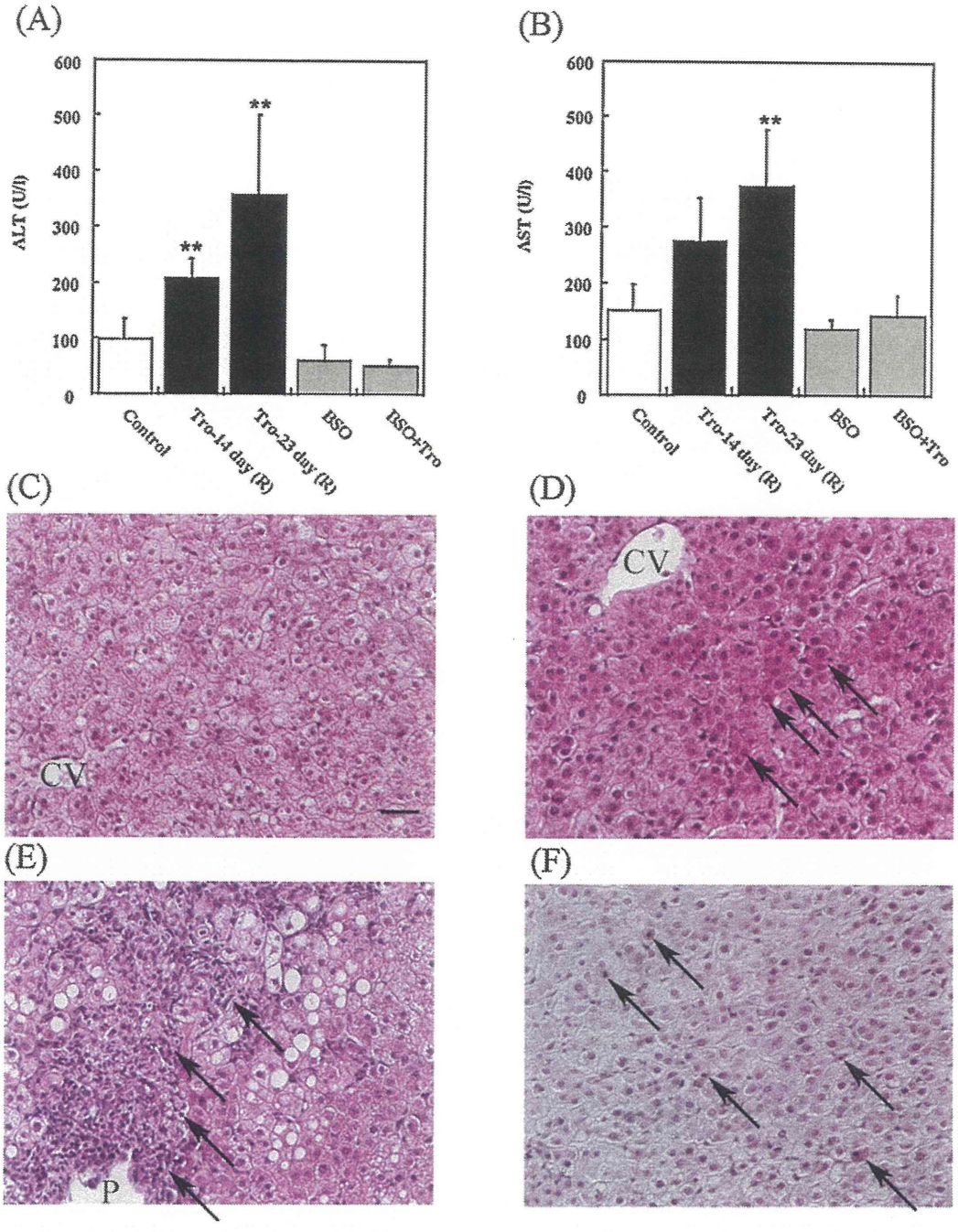

Fig. 1. Changes in the serum ALT and AST levels and liver histology by Tro and/or BSO administration in chimeric mice. The chimeric mice were orally administered Tro (1000 mg/kg/10 ml, suspended in 0.5% CMC) once daily for 14 or 23 days in a non-fasting condition, and 0.5% CMC was administered once daily for 14 days as a control. BSO (10 mM in drinking water) was also given alone or with Tro administration for 14 days. (A) ALT and (B) AST were measured 24 h after the last administration. The data are shown as the mean ± SD of the results from 3 to 6 mice. In the Tro-14 day ($n = 3$) and Tro-23 day ($n = 3$) group, the data are from the responder chimeric mice (R). The differences compared to the control group ($n = 6$) were considered significant at $^{**}P < 0.01$. (C–F) The liver specimens from the chimeric mice were sampled 24 h after the last Tro administration and subsequently stained with H&E. The human hepatocytes in the control chimeric mouse had a clear cytoplasm and no cellular infiltration (C, mouse no. 2). The arrows indicate an eosinophilic change of human hepatocytes (D, mouse no. 12, Responder), neutrophil infiltration (E, mouse no. 13, Responder) and necrosis of human hepatocytes (F, mouse no. 14, Responder). CV: central vein; P: portal vein; Bars: 40 μm (C–F are the same scale).

In the control chimeric mouse, a clear cytoplasm and no cellular infiltration were observed in the human hepatocytes in the liver tissue of the chimeric mice (Fig. 1C). In the responder chimeric mice, the human hepatocytes in the liver tissue showed slight eosinophilic changes (Fig. 1D), neutrophil infiltration surrounding the area of the portal vein (Fig. 1E) and scattered single cell necrosis (Fig. 1F) after Tro administration.

3.2. Oxidative stress responses in chimeric mice with a humanized liver

In both the Tro 1000-14 day and Tro 1000-23 day groups, the hepatic GSH contents were significantly higher in the Tro-administered responder mice by approximately 2-fold than in the control group (Fig. 2A). GST activities, SOD2 activities and the

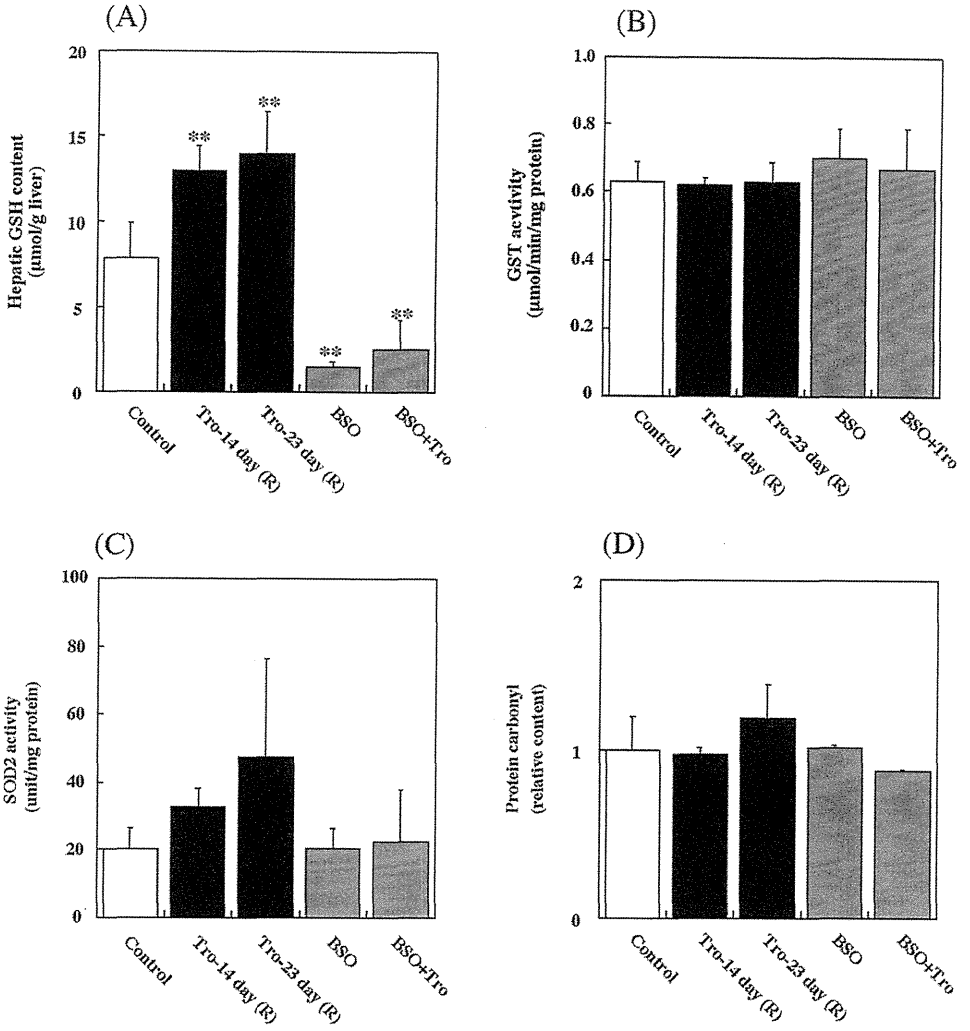

Fig. 2. Changes in the hepatic GSH content (A), GST activity (B), SOD2 activity (C), and plasma protein carbonyl content (D) in the chimeric mice that were administered Tro and/or BSO. The data are shown as the mean ± SD of the results from 3 to 6 mice. In the Tro-14 day and Tro-23 day groups, the data are from the responder chimeric mice. The differences compared to the control group were considered significant at $^{**}P < 0.01$.

protein carbonyl content showed no significant change following Tro administration (Fig. 2B–D). SOD2 activity in the Tro 1000-23 day group was higher than in the control: however, the difference in activity was not significant.

The effects of the GSH-lowering agent BSO on oxidative stress in the chimeric mice were evaluated. The hepatic GSH contents were significantly decreased in the BSO group by approximately 0.2-fold compared to the control group. However, in the BSO and Tro-administered group, the GSH content was suppressed by Tro administration. The hepatic GST activities were unchanged with the administration of BSO alone or BSO and Tro administration. The administration of BSO and Tro showed no change in SOD2 activity. The protein carbonyl contents also showed no change among the groups in this study (Fig. 2D). These results suggested that Tro induced the GSH synthesis enzyme, which was inhibited by BSO.

3.3. Effect of Tro and/or BSO administration on the expression of drug metabolizing enzymes in the chimeric mice with a humanized liver

We determined the expression levels of drug metabolizing enzymes, which are involved in the metabolism of Tro in human. The expression level of human CYP2C8 mRNA (Fig. 3A) was increased with the administration of Tro and/or BSO. The expression level of CYP2C8 protein (Fig. 3B) and paclitaxel 6a-hydroxylase activities (Fig. 3C) were significantly increased by the administration of Tro. The expression levels of CYP3A4 mRNA (Fig. 4A) and protein (Fig. 4B) also tended to increase with the administration of Tro and/or BSO. Dexamethasone 6-hydroxylase activities were significantly increased by the administration of Tro and/or BSO. Therefore, these results clearly demonstrated that Tro induced CYP2C8 and CYP3A4 in the liver of the chimeric mice with a humanized liver. Interestingly, the administration of BSO alone also induced both enzymes. Based on these data, enzyme induction is unlikely to be involved in Tro-induced liver injury. In addition, we found that Tro induced the expression level of human UGT1A1 (Fig. 5B) mRNA. The administration of BSO and/or Tro also induced the expression level of UGT1A1 mRNA.

4. Discussion

During the preclinical development and following the withdrawal of Tro, pharmaceutical companies performed numerous toxicity studies using mice, rats and monkeys (Watanabe et al.,

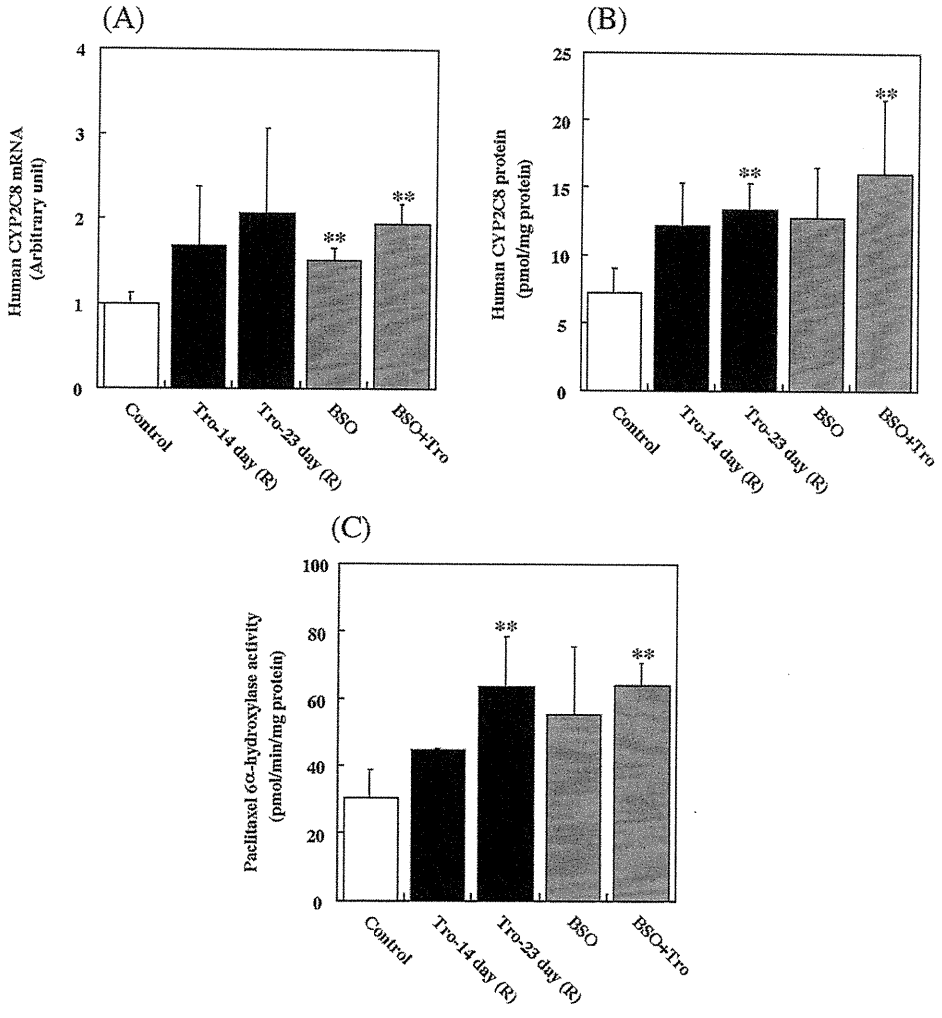

Fig. 3. Changes in the expression level of human CYP2C8 mRNA (A), protein content (B), and enzyme activity (C) in the liver of chimeric mice that were administered Tro and/or BSO. Paclitaxel 6a-hydroxylase activity was catalyzed by CYP2C8 and measured using 20 μM paclitaxel as a substrate. The data are shown as the mean ± SD of the results from 3 to 6 mice. In the Tro-14 day and Tro-23 day groups, the data are from the responder chimeric mice. The differences compared to the control group were considered significant at $^{**}P < 0.01$.

1999). In these toxicity studies, Tro was administered at a dose of 800 mg/kg/day for 24 months to mice, 1200 mg/kg/day for 12 months to rats and 1200 mg/kg/day for 12 months to monkeys, but no signs of liver dysfunction were confirmed (Watanabe et al., 1999). Chimeric mice with a humanized liver are suitable for *in vivo* studies utilizing human hepatocytes. The present study used chimeric mice with a humanized liver and successfully demonstrated Tro-induced liver with the once daily oral administration for 14 and 23 days of 1000 mg/kg Tro. The development of Tro-induced liver injuries in the responder chimeric mice was confirmed by the significant increase in the final serum ALT and AST levels that occurred in an administration-duration-dependent manner (Fig. 1A and B), the eosinophilic changes (Fig. 1D) and cellular infiltrations in the liver tissue (Fig. 1E) and single cell necrosis of human hepatocytes (Fig. 1F). Using the same chimeric mice, Schulz-Utermoehl et al. (2012) did not demonstrate liver injury administering a once daily oral dose for 7 days of 300 and 600 mg/kg Tro, and no significant differences in the pharmacokinetics parameters of C_{max} or AUC were observed following doses of Tro at 300 and 600 mg/kg. These evidences support our results that 250 and 500 mg/kg of Tro was insufficient for the onset of Tro-induced liver injury in the chimeric mice when dosed once daily for 28 days. Both the dose level and the dosing period will be essential factors for the onset of Tro-induced liver injury.

The increase of serum transaminases was considered to be derived from the human hepatocytes, which was supported by the histological changes. However, we were unable to distinguish human ALT from mouse ALT quantitatively (data not shown). Conversely, two out of five mice in the Tro 1000-14 day group and one out of four mice in the Tro 1000-23 day group did not show hepatic injury. As shown in Table 1, the chimeric mice exhibited a hAlb concentration of 8.0–14.9 mg/ml and 75–92% of RI and received transplanted human hepatocytes from the same donor. The hAlb levels of the non-responder chimeric mice ranged from 8.2 (RI: 75%) to 11.7 mg/ml (RI; 85%), and appeared to not be critically different from the hAlb levels of the responder chimeric mice, which ranged from 9.0 (RI: 78%) to 14.9 (RI: 92%). Therefore, it was considered that the individual difference in the onset of liver injury among the mice would depend on other factors as discussed below.

It has been reported that the double null mutant of GSTT1 and GSTM1 in humans correlated with Tro-associated abnormal increases in ALT levels (odds ratio, 3.692; 95% confidence interval, 1.354–10.066; $P = 0.008$) (I. Watanabe et al., 2003). However, the present study revealed that the difference in the onset of liver injury

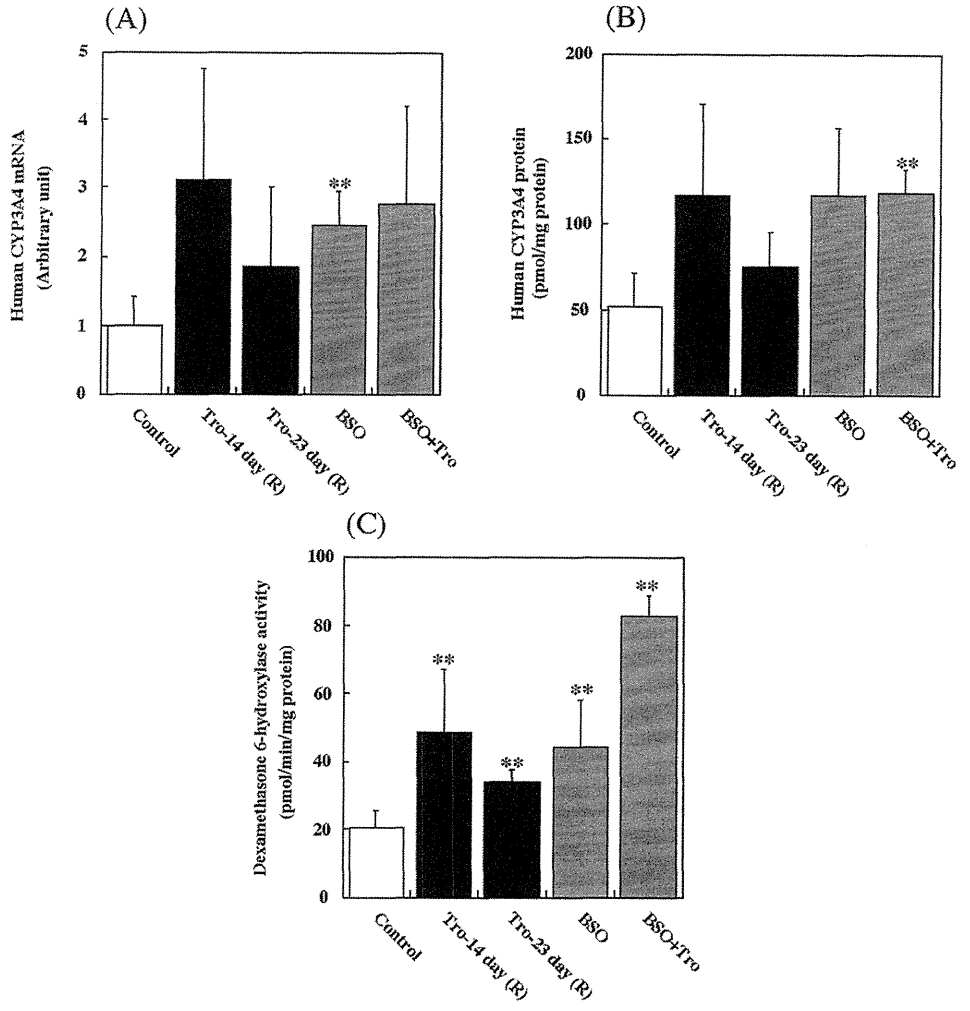

Fig. 4. Changes in the expression level of human CYP3A4 mRNA (A), protein content (B), and enzyme activity (C) in the liver of chimeric mice administered Tro and/or BSO. Dexamethasone 6-hydroxylase activity was catalyzed by CYP3A4 and measured using 100 μM dexamethasone as a substrate. The data are shown as the mean ± SD of the results from 3 to 6 mice. In the Tro-14 day and Tro-23 day groups, the data are from the responder chimeric mice. The differences compared to the control group were considered significant at $^{**}P < 0.01$.

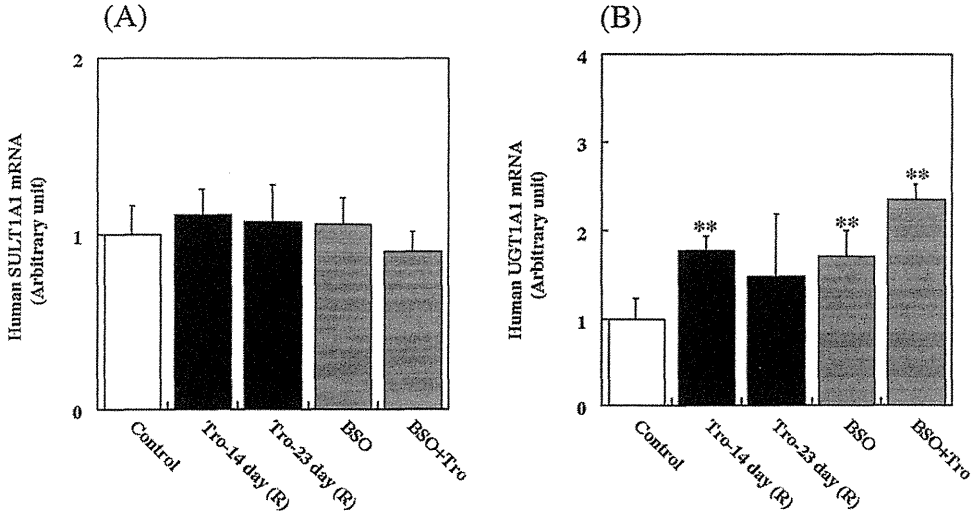

Fig. 5. Changes in the expression level of human SULT1A1 mRNA (A) and human UGT1A1 mRNA expression (B) in the liver of chimeric mice that were administered Tro and/or BSO. The data are shown as the mean ± SD of the results from 3 to 6 mice. In the Tro-14 day and Tro-23 day groups, the data are from the responder chimeric mice. The differences compared to the control group were considered significant at $^{**}P < 0.01$.

could be Tro-induced in the chimeric mice with genetically identical human hepatocytes genotyped to wild-type GSTT1 and GSTM1 (data not shown). It is conceivable that the double null mutant of GSTT1 and GSTM1 is unlikely to be a risk factor, which was recently suggested by Usui et al. (2011) using cytotoxicity assays of human hepatocytes.

BSO was administered to evaluate the effects of GSH depletion on Tro-induced liver injury. The suspected active metabolite of Tro, a quinone metabolite, has been reported to not react directly with GSH, and it can be further metabolized to an *O*-quinone methide or undergo ring opening to produce additional highly electrophilic intermediates (Kassahun et al., 2001). However, in this study, neither the serum biochemical analyses nor the histological examinations showed evidence of liver injury in the BSO alone and BSO- and Tro-administered group, whereas the hepatic GSH contents decreased approximately 0.2- and 0.4-fold in these groups, respectively compared to the control group (Fig. 2A). Furthermore, hepatic GST activities were maintained in all groups (Fig. 2B). Although the results in this study appear to not support the general understanding of scavenging systems for reactive metabolites, it was suggested that the onset of Tro-induced liver injury was independent of scavenging systems associated with hepatic GSH. Interestingly, the hepatic GSH contents significantly increased with the administration of Tro (Fig. 2A), although the functional mechanism in relation to the onset of liver injury was unclear.

SOD2 activity and protein carbonyl contents were measured to clarify whether an increase in oxidative stress might be associated with the onset of Tro-induced liver injury (Fig. 2C and D), as reported in a study using *SOD2*$^{+/-}$ mice (Ong et al., 2007). In the *SOD2*$^{+/-}$ mouse study, the increase in the serum AST level and the degeneration of hepatocytes were observed when 30 mg/kg of Tro was intraperitoneally administered once per day for 4 weeks (Ong et al., 2007). However, the phenomenon was not reproduced by other group (Fujimoto et al., 2009) despite the administered to the same dose to the same *SOD2*$^{+/-}$ mice. We found that SOD2 activities were tended to increase in the Tro-23 day group. Furthermore, the protein carbonyl contents were unchanged. These results suggest that oxidative stress may not involved in Tro-induced liver injury in the chimeric mice.

In humans, Tro is metabolized by three pathways, *i.e.*, sulfation by SULT1A1 (Honma et al., 2002), glucuronidation by UGT1A1 (Yoshigae et al., 2000), and oxidation to form a quinone metabolite (M3) by CYP2C8 and CYP3A4 (Yamazaki et al., 1999; Yamamoto et al., 2002). Recently, the chimeric mice were confirmed to show the unique profiles in metabolism of Tro when compared to SCID mice (Schulz-Utermoehl et al., 2012). A total of 32 putative metabolites plus Tro were detected in blood from the chimeric mice, with 14 (M1, M4–M10, M12 and M17–M21) of these metabolites detected only in blood from the chimeric mice. Of these 14 metabolites, 4 (M4, M7, M8 and M12) were also detected only in liver extracts from the chimeric mice. The relative concentrations of the glucuronide metabolite (M13) were higher in liver preparations from SCID mice. These findings suggested the chimeric mice possess metabolically active human hepatocytes and have a potential to generate unique human metabolite (Schulz-Utermoehl et al., 2012). The involvement of a sulfo-conjugate in Tro-induced liver injury was suggested in *in vitro* study by Saha et al. (2010) who reported that a sulfo-conjugate of Tro exerted direct toxic effects on human hepatocytes, possibly *via* oxidative stress induction. In contract, the expression level of SULT1A1 mRNA was not changed in this study, suggesting the difference effect of Tro between *in vivo* and *in vitro* study.

We found that CYP2C8 and CYP3A4 were induced by the administration of Tro, as previously reported (Sahi et al., 2003). However, the onset of the Tro-induced liver injury was considered independent of the induction of these drug-metabolizing enzymes because enzyme induction was also observed in the BSO alone- and BSO and Tro-administered group. The cause of the moderate induction of CYP3A4 in the Tro-23 day group compared with the Tro-14 day group remains unclear. However, it was reported that hepatic expression levels of proinflammatory cytokines, tumor necrosis factor (TNF) α and interleukin (IL)-6 and chemokines were increased in the mouse model of drug-induced liver injury (Toyoda et al., 2011, 2012). TNFα was also identified to be involved in the down-regulation of CYP3A11 and CYP3A25 in mouse liver (Kinloch et al., 2011). In addition, IL-6 was reported to down-regulate the expression of CYP3A4 *via* pregnane X receptor in human hepatocytes (Yang et al., 2010). Taking these recent reports into consideration, chronic hepatic inflammation in the Tro-23 day group might be a causal factor for the decreased expression level of CYP3A4 in this study.

As shown in Fig. 5B, UGT1A1 appears unrelated to the onset of the Tro-induced liver injury because significant increases in human UGT1A1 mRNA expression were observed not only in the Tro-14 day group but also in the BSO alone and BSO- and Tro-administered groups.

Notably, the chimeric mice were generated using an uPA$^{+/+}$/SCID mouse line, which is defective in functional T and B lymphocytes (Bosma et al., 1983). Tro-induced liver injury in the chimeric mice could be successfully produced when free from T and B lymphocyte-mediated immune responses. However, SCID mice were once daily orally administered Tro at 300 and 600 mg/kg doses for 7 days and showed no change in ALT and AST levels (Schulz-Utermoehl et al., 2012). Further investigations comparing SCID mice and the chimeric mice with a humanized liver are necessary.

Idiosyncratic liver injury is a critical issue for clinical practice and drug development. Thus, numerous attempts have been made to establish a method for predicting idiosyncratic liver injury in human. The present study succeeded in demonstrating Tro-induced liver injury using chimeric mice with a humanized liver. The advantage of this mouse model is to enable human hepatocytes to be examined in an *in vivo* environment. The chimeric mice with a humanized liver will be a useful tool to investigate the unsolved mechanism of idiosyncratic Tro-induced hepatic injury.

Funding information

Health and Labor Sciences Research Grants from the Ministry of Health, Labor, and Welfare of Japan (H23-BIO-G001).

Conflict of interest statement

The authors declare that there are no conflicts of interest.

References

Bedoucha, M., Atzpodien, E., Boelsterli, U.A., 2001. Diabetic KKAy mice exhibit increased hepatic PPARγ1 gene expression and develop hepatic steatosis upon chronic treatment with antidiabetic thiazolidinediones. Journal of Hepatology 35, 17–23.

Bosma, G.C., Custer, R.P., Bosma, M.J., 1983. A severe combined immunodeficiency mutation in the mouse. Nature 301, 527–530.

Fujimoto, K., Kumagai, K., Ito, K., Arakawa, S., Ando, Y., Oda, S., Yamoto, T., Manabe, S., 2009. Sensitivity of liver injury in heterozygous Sod2 knockout mice treated with troglitazone or acetaminophen. Toxicologic Pathology 37, 193–200.

Habig, W.H., Pabst, M.J., Jakoby, W.B., 1974. Glutathione S-transferases. The first enzymatic step in mercapturic acid formation. Journal of Biological Chemistry 249, 7130–7139.

He, K., Talaat, R.E., Pool, W.F., Reily, M.D., Reed, J.E., Bridges, A.J., Woolf, T.F., 2004. Metabolic activation of troglitazone: identification of a reactive metabolite and mechanisms involved. Drug Metabolism and Disposition: The Biological Fate of Chemicals 32, 639–646.

Honma, W., Shimada, M., Sasano, H., Ozawa, S., Miyata, M., Nagata, K., Ikeda, T., Yamazoe, Y., 2002. Phenol sulfotransferase, ST1A3, as the main enzyme catalyzing sulfation of troglitazone in human liver. Drug Metabolism and Disposition: The Biological Fate of Chemicals 30, 944–949.

Izukawa, T., Nakajima, M., Fujiwara, R., Yamanaka, H., Fukami, T., Takamiya, M., Aoki, Y., Ikushiro, S., Sakaki, T., Yokoi, T., 2009. Quantitative analysis of UDP-glucuronosyltransferase (UGT) 1A and UGT2B expression levels in human livers. Drug Metabolism and Disposition: The Biological Fate of Chemicals 37, 1759–1768.

Jia, D.M., Tabaru, A., Akiyama, T., Abe, S., Otsuki, M., 2000. Troglitazone prevents fatty changes of the liver in obese diabetic rats. Journal of Gastroenterology and Hepatology 15, 1183–1191.

Kassahun, K., Pearson, P.G., Tang, W., McIntosh, I., Leung, K., Elmore, C., Dean, D., Wang, R., Doss, G., Baillie, T.A., 2001. Studies on the metabolism of troglitazone to reactive intermediates in vitro and in vivo. Evidence for novel biotransformation pathways involving quinone methide formation and thiazolidinedione ring scission. Chemical Research in Toxicology 14, 62–70.

Katoh, M., Matsui, T., Nakajima, M., Tateno, C., Kataoka, M., Soeno, Y., Horie, T., Iwasaki, K., Yoshizato, K., Yokoi, T., 2004. Expression of human cytochromes P450 in chimeric mice with humanized liver. Drug Metabolism and Disposition: The Biological Fate of Chemicals 32, 1402–1410.

Katoh, M., Matsui, T., Okumura, H., Nakajima, M., Nishimura, M., Naito, S., Tateno, C., Yoshizato, K., Yokoi, T., 2005. Expression of human phase II enzymes in chimeric mice with humanized liver. Drug Metabolism and Disposition: The Biological Fate of Chemicals 33, 1333–1340.

Katoh, M., Sawada, T., Soeno, Y., Nakajima, M., Tateno, C., Yoshizato, K., Yokoi, T., 2007. In vivo drug metabolism model for human cytochrome P450 enzyme using chimeric mice with humanized liver. Journal of Pharmaceutical Sciences 96, 428–437.

Kinloch, R.D., Lee, C.M., van Rooijen, N., Morgan, E.T., 2011. Selective role for tumor necrosis factor-α, but not interleukin-1 or Kupffer cells, in down-regulation of CYP3A11 and CYP3A25 in livers of mice infected with a noninvasive intestinal pathogen. Biochemical Pharmacology 82, 312–321.

Nishimura, M., Yoshitsugu, H., Yokoi, T., Tateno, C., Kataoka, M., Horie, T., Yoshizato, K., Naito, S., 2005. Evaluation of mRNA expression of human drug-metabolizing enzymes and transporters in chimeric mouse with humanized liver. Xenobiotica 35, 877–890.

Ong, M.M., Latchoumycandane, C., Boelsterli, U.A., 2007. Troglitazone-induced hepatic necrosis in an animal model of silent genetic mitochondrial abnormalities. Toxicological Sciences 97, 205–213.

Saha, S., New, L.S., Ho, H.K., Chui, W.K., Chan, E.C.Y., 2010. Direct toxicity effects of sulfo-conjugated troglitazone on human hepatocytes. Toxicology Letters 195, 135–141.

Sahi, J., Black, C.B., Hamilton, G.A., Zheng, X., Jolley, S., Rose, K.A., Gilbert, D., LeCluyse, E.L., Sinz, M.W., 2003. Comparative effects of thiazolidinediones on in vitro P450 enzyme induction and inhibition. Drug Metabolism and Disposition: The Biological Fate of Chemicals 31, 439–446.

Schulz-Utermoehl, T., Sarda, S., Foster, J.R., Jacobsen, M., Kenna, J.G., Morikawa, Y., Salmu, J., Gross, G., Wilson, I.D., 2012. Evaluation of the pahrmacokinetics, biotransformation, and hepatic transporter effects of troglitazone in mice with humanized livers. Xenobiotica 42, 503–517.

Tateno, C., Yoshizane, Y., Saito, N., Kataoka, M., Utoh, R., Yamasaki, C., Tachibana, A., Soeno, Y., Asahina, K., Hino, H., Asahara, T., Yokoi, T., Furukawa, T., Yoshizato, K., 2004. Near completely humanized liver in mice shows human-type metabolic responses to drugs. American Journal of Pathology 165, 901–912.

Tettey, J.N., Maggs, J.L., Rapeport, W.G., Pirmohamed, M., Park, B.K., 2001. Enzyme induction dependent bioactivation of troglitazone and troglitazone quinone in vivo. Chemical Research in Toxicology 14, 965–974.

Tietze, F., 1969. Enzymatic method for quantitative determination of nanogram amounts of total and oxidized glutathione: applications to mammalian blood and other tissues. Analytical Biochemistry 27, 502–522.

Tomlinson, E.S., Maggs, J.L., Park, B.K., Back, D.J., 1997. Dexamethasone metabolism in vitro: species differences. Journal of Steroid Biochemistry and Molecular Biology 62, 345–352.

Toyoda, Y., Miyashita, T., Endo, S., Tsuneyama, K., Fukami, T., Nakajima, M., Yokoi, T., 2011. Estradiol and progesterone modulate halothane-induced liver injury in mice. Toxicology Letters 204, 17–24.

Toyoda, Y., Endo, S., Tsuneyama, K., Miyashita, T., Yano, A., Fukami, T., Nakajima, M., Yokoi, T., 2012. Mechanism of exacerbative effect of progesterone on drug-induced liver injury. Toxicological Sciences 126, 16–27.

Usui, T., Hashizume, T., Katumata, T., Yokoi, T., Komuro, S., 2011. In vitro investigation of the glutathione transferase M1 and T1 null genotypes as risk factors for troglitazone-induced liver injury. Drug Metabolism and Disposition: The Biological Fate of Chemicals 39, 1303–1310.

Watanabe, T., Ohashi, Y., Yasuda, M., Takaoka, M., Furukawa, T., Yamoto, T., Sanbuissho, A., Manabe, S., 1999. Was it not possible to predict liver dysfunction caused by troglitazone during the nonclinical safety studies? Reevaluation of Safety 30, 537–546.

Watanabe, T., Furukawa, T., Sharyo, S., Ohashi, Y., Yasuda, M., Takaoka, M., Manabe, S., 2000. Effect of troglitazone on the liver of a Gunn rat model of genetic enzyme polymorphism. Journal of Toxicological Sciences 25, 423–431.

Watanabe, I., Tomita, A., Shimizu, M., Sugawara, M., Yasumo, H., Koishi, R., Takahashi, T., Miyoshi, K., Nakamura, K., Izumi, T., Matusshita, Y., Furukawa, H., Haruyama, H., Koga, T., 2003. A study to survey susceptible genetic factors responsible for troglitazone-associated hepatotoxicity in Japanese patients with type 2 diabetes mellitus. Clinical Pharmacology and Therapeutics 73, 435–455.

Watanabe, T., Sagisaka, H., Arakawa, S., Shibaya, Y., Watanabe, M., Igarashi, I., Tanaka, K., Totsuka, S., Takasaki, W., Manabe, S., 2003. A novel model of continuous depletion of glutathione in mice treated with L-buthionine (S, R)-sulfoximine. Journal of Toxicological Sciences 28, 455–469.

Willey, T.A., Bekos, E.J., Gaver, R.C., Duncan, G.F., Tay, L.K., Beijnen, J.H., Farmen, R.H., 1993. High-performance liquid chromatographic procedure for the quantitative determination of paclitaxel (Taxol) in human plasma. Journal of Chromatography 621, 231–238.

Yamamoto, Y., Yamazaki, H., Ikeda, T., Watanabe, T., Iwabuchi, H., Nakajima, M., Yokoi, T., 2002. Formation of a novel quinone epoxide metabolite of troglitazone with cytotoxicity to HepG2 cells. Drug Metabolism and Disposition: The Biological Fate of Chemicals 30, 155–160.

Yamazaki, H., Shibata, A., Suzuki, M., Nakajima, M., Shimada, N., Guengerich, F.P., Yokoi, T., 1999. Oxidation of troglitazone to a quinone-type metabolite catalyzed by cytochrome P-450 2C8 and P-450 3A4 in human liver microsomes. Drug Metabolism and Disposition: The Biological Fate of Chemicals 27, 1260–1266.

Yang, J., Hao, C., Yang, D., Shi, D., Song, X., Luan, X., Hu, G., Yan, G., 2010. Pregnane X receptor is required for interleukin-6-mediated down-regulation of cytochrome P450 3A4 in human hepatocytes. Toxicology Letters 197, 219–226.

Yoshigae, Y., Konno, K., Takasaki, W., Ikeda, T., 2000. Characterization of UDP-glucuronosyltransferases (UGTs) involved in the metabolism of troglitazone in rats and humans. Journal of Toxicological Sciences 25, 433–441.

Yoshikawa, Y., Morita, M., Hosomi, H., Tsuneyama, K., Fukami, T., Nakajima, M., Yokoi, T., 2009. Knockdown of superoxide dismutase 2 enhances acetaminophen-induced hepatotoxicity in rat. Toxicology 264, 89–95.

TOXICOLOGICAL SCIENCES 130(1), 4–16 (2012)
doi:10.1093/toxsci/kfs222
Advance Access publication July 12, 2012

Metabolic Activation and Inflammation Reactions Involved in Carbamazepine-Induced Liver Injury

Satonori Higuchi,* Azusa Yano,* Shohei Takai,* Koichi Tsuneyama,† Tatsuki Fukami,* Miki Nakajima,* and Tsuyoshi Yokoi*,[1]

*Drug Metabolism and Toxicology, Faculty of Pharmaceutical Sciences, Kanazawa University, Kanazawa 920–1192, Japan; and †Department of Diagnostic Pathology, Graduate School of Medicine and Pharmaceutical Science for Research, University of Toyama, Toyama 930-0194, Japan

[1]To whom correspondence should be addressed. Fax: +81-76-234-4407. E-mail: tyokoi@p.kanazawa-u.ac.jp.

Received May 17, 2012; accepted July 3, 2012

Drug-induced liver injury is a major safety concern in drug development and clinical pharmacotherapy; however, advances in the understanding of the mechanisms of drug-induced liver injury are hampered by the lack of animal models. Carbamazepine (CBZ) is a widely used antiepileptic agent. Although the drug is generally well tolerated, only a small number of patients prescribed CBZ develop severe hepatitis. In the present study, we developed a mouse model of CBZ-induced liver injury and elucidated the mechanisms accounting for the hepatotoxicity of CBZ. Male BALB/c mice were orally administered CBZ for 5 days. The plasma levels of alanine aminotransferase and aspartate aminotransferase were prominently increased, and severe liver damage was observed via histological evaluation. The analysis of the plasma concentration of CBZ and its metabolites demonstrated that 3-hydroxy CBZ may be relevant in CBZ-induced liver injury. The hepatic glutathione levels were significantly decreased, and oxidative stress markers were significantly altered. Mechanistic investigations found that hepatic mRNA levels of toll-like receptor 4, receptor for advanced glycation end products, and their ligands were significantly increased. Moreover, the plasma concentrations of proinflammatory cytokines were also increased. Prostaglandin E_1 administration ameliorated the hepatic injury caused by CBZ. In conclusion, metabolic activation followed by the stimulation of immune responses was demonstrated to be involved in CBZ-induced liver injury in mice.

Key Words: **carbamazepine; IL-17; hepatotoxicity; metabolism; mouse model.**

Adverse drug reactions are a clinical concern and cause attrition in drug development, with hepatotoxicity being a major contributor. It is thought that many idiosyncratic drug reactions result from the production of reactive metabolites by cytochrome P450 (CYP) enzyme systems. The reactive metabolites may lead to hepatic injuries either by direct or by immune-related mechanisms (Park *et al.*, 2000).

Carbamazepine (CBZ) is a widely used antiepileptic agent. Although the drug is generally well tolerated, only a limited number of patients prescribed CBZ develop severe, potentially life-threatening idiosyncratic reactions such as agranulocytosis, hepatitis, and Stevens-Johnson syndrome (Björnsson and Olsson, 2005; Kaufman and Shapiro, 2000; Pallock, 1987). The reasons why only few individuals are affected are poorly understood. Serious CBZ-associated hepatotoxicity assumes the following two forms: (1) a hypersensitive reaction in the form of granulomatous hepatitis that presents with fever and abnormal liver functions and (2) an acute hepatitis and hepatocellular necrosis with fever and inflammation (Björnsson, 2008; Björnsson and Olsson, 2005). In addition, the presence of a specific autoantibody directed against a human liver microsomal protein in a patient who had severe hepatotoxicity with CBZ has been reported (Pirmohamed *et al.*, 1992a). Based on these reports, the liver injury associated with CBZ is thought to have an immunoallergic basis. In contrast, another antiepileptic drug, oxcarbazepine (OXC), is not likely to be associated with idiosyncratic hepatotoxicity in humans, and there have been only a few case reports showing mild or transitory liver injury (Ahmed and Siddiqi, 2006; Björnsson, 2008).

CBZ is extensively metabolized in humans to over 30 metabolites, and the most important pathway involves the formation of the stable CBZ-10,11-epoxide followed by hydroxylation to CBZ-10,11-*trans*-dihydroxy (diOH) (Lertratanangkoon and Horning, 1982; Lu and Uetrecht, 2008). Chemically reactive metabolites are also generated as shown in Figure 1. Numerous studies have assayed CBZ-induced cytotoxicity by reactive metabolites *in vitro*, and they have suggested that CBZ 2,3-epoxide and 3-hydroxy (OH) CBZ might play a role in CBZ-induced idiosyncratic drug reactions via covalent binding to the protein or the production of reactive oxygen species (ROS) (Lu and Uetrecht, 2008; Pirmohamed *et al.*, 1992b), and glutathione (GSH) and microsomal epoxide hydrolase are involved in detoxification (Pirmohamed *et al.*, 1992b). However, there are no reports of CBZ-induced hepatotoxicity in an *in vivo* animal model.

It is well known that ROS is involved in drug-induced liver injury via mitochondrial dysfunction or hepatocyte necrosis (Jaeschke *et al.*, 2002), and it was recently reported that ROS increased the expression of the toll-like receptor (TLR) and the

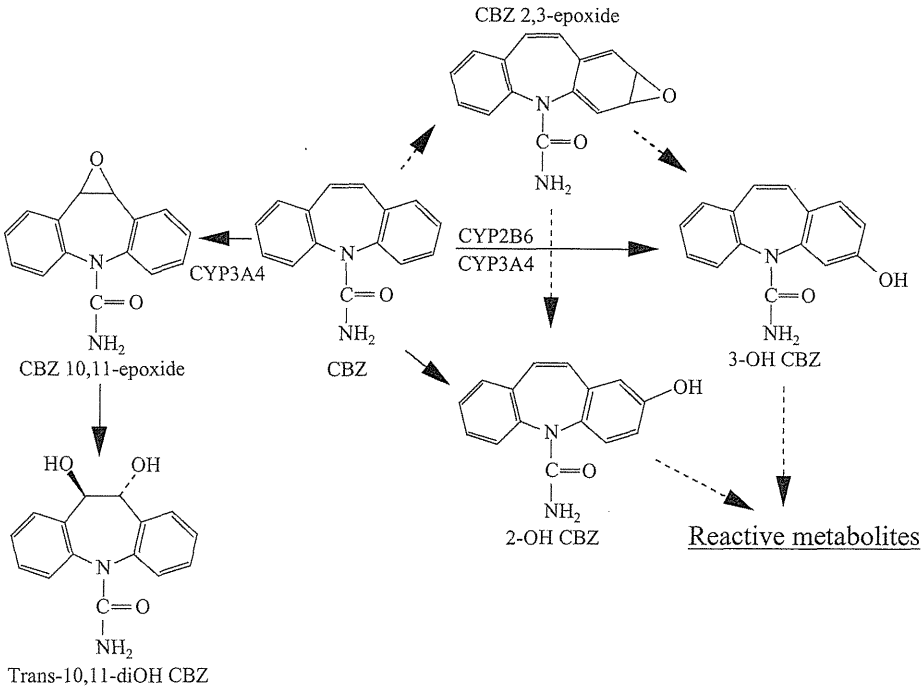

FIG. 1. The metabolic pathways of CBZ.

receptor for advanced glycation end products (RAGE), as well as their ligands, such as S100 protein and high-mobility group box 1 (HMGB1) (Yao and Brownlee, 2010). The activation of TLR or RAGE results in the induction of inflammatory cytokines and chemokines (Lotze *et al.*, 2007). Cytokines and chemokines, followed by inflammation or the infiltration of lymphocytes to hepatocytes, are involved in immune-mediated hepatotoxicity, and they are predominantly secreted from immune cells such as T lymphocytes and macrophages (Kita *et al.*, 2001; Oo and Adams, 2009). Cytokines are generated by several transcriptional factors: T-box expressed in T cells (T-bet) induces the secretion of interferon (IFN)-γ and interleukin (IL)–12; GATA-binding domain-3 (GATA-3) induces IL-4, IL-5, and IL-13 production; and retinoid-related orphan receptor (ROR)-γt promotes the production of IL-6 and IL-23, which leads to an increase in IL-17 generation (Kidd, 2003; Langrish *et al.*, 2005; Steinman, 2007).

IL-17, a T helper (Th) 17-type cytokine, acts as a potent inflammatory cytokine, and it is detected in sera and target tissues of patients with various immune-related diseases, including rheumatoid arthritis, multiple sclerosis, systemic lupus erythematosus, and asthma (Kidd, 2003; Steinman, 2007). Consistent with those observations, it has been suggested that IL-17 is involved in the pathogenesis of immune-mediated hepatotoxicities in mice, such as halothane- or α-naphthylisothiocyanate-induced hepatotoxicity (Kobayashi *et al.*, 2009, 2010).

At present, the widely studied model of drug-induced liver injury is the acetaminophen (APAP)-induced liver injury model, which commonly involves mice as the model organism. Although important information on the mechanisms of drug-induced acute inflammatory injury has been generated from this model, APAP hepatotoxicity does not encompass all possible mechanistic features of drug-induced liver injury. Therefore, it is critical to establish several animal models of drug-induced liver injury. This work is the first study to establish a mouse model of CBZ-induced hepatotoxicity. Our data suggest that metabolic activation and inflammation reactions are involved in CBZ-induced liver injury, and this is an appropriate animal model for the study of the severe hepatotoxicity induced by CBZ.

MATERIALS AND METHODS

Materials. CBZ was purchased from Wako Pure Chemical Industries (Osaka, Japan). OXC was from LKT Laboratories (St Paul, Minnesota), and 2-OH CBZ and 3-OH CBZ were from Toronto Research Chemicals (Toronto, Canada). CBZ-10, 11-epoxide and trans-10, 11-diOH CBZ were kindly provided by Novartis Pharma Inc. (Basel, Switzerland). RNAiso was from Nippon Gene (Tokyo, Japan). Fuji DRI-CHEM slides of GPT/ALT-PIII and GOT/AST-PIII used to measure alanine aminotransferase (ALT) and aspartate aminotransferase (AST), respectively, were purchased from Fujifilm (Tokyo, Japan). ReverTra Ace was from Toyobo (Tokyo, Japan). Random hexamers and SYBR Premix Ex Taq were from Takara (Osaka, Japan). All primers were commercially synthesized at Hokkaido System Sciences (Sapporo, Japan). Eritoran was kindly provided by Eisai Co. (Tokyo, Japan). Prostaglandin E_1 (PGE_1) was purchased from Nippon Chemiphar (Tokyo, Japan). The monoclonal anti-mouse IL-17 antibody, monoclonal anti-mouse/rat RAGE antibody, and monoclonal rat IgG2a isotype, used as a control, were from R&D Systems (Abingdon, UK). The rabbit polyclonal antibody against myeloperoxidase (MPO) was from DAKO (Carpinteria, CA). The Ready-SET-GO! Mouse IL-17 ELISA kit and the Mouse IL-23 ELISA kit were from eBioscience (San Diego, CA). The HMGB1 ELISA kit II was from Sino-Test Corporation (Tokyo, Japan). Other chemicals were of analytical or the highest grade commercially available.

CBZ and OXC administration. Male BALB/cCrSlc mice (8–10 weeks old, 22–27 g) were obtained from SLC Japan (Hamamatsu, Japan). Mice were housed in a controlled environment (temperature 23 ± 1°C, humidity 50 ± 10%, and 12-h light/12-h dark cycle) in the institution's animal facility with *ad libitum* access to food and water. Animals were acclimatized before use in the experiments. Mice were orally administered CBZ (in corn oil) at a dose of 400 mg/kg for 4 days and 400 to 800 mg/kg on the 5th day. As a control, mice were administered OXC at a dose of 400 mg/kg for 4 days and 800 mg/kg on the 5th day. This dosing regimen is termed "method A" in the following studies. At 1.5, 3, 6, 12, 24, 48, and 72 h after the last administration, the blood and the liver were collected. During a repeated administration study, body weight was recorded. In the single administration study, mice were administered 400 mg/kg or 800 mg/kg CBZ and were sacrificed at 3 h (for assay of the plasma concentration of CBZ and its metabolites) or 24 h (for measurement of the ALT level) after administration. A portion of each excised liver was fixed in 10% formalin neutral buffer solution and used for immunohistochemical staining. The degree of liver injury was assessed by hematoxylin and eosin (H&E) staining, and ALT and AST levels were measured by a DRI-CHEM (Fujifilm). Animal maintenance and treatment were conducted in accordance with the National Institutes of Health Guide for Animal Welfare of Japan, and the protocols were approved by the Institutional Animal Care and Use Committee of Kanazawa University, Japan.

Treatment with Cyp3a inhibitors. One hour before the last CBZ administration, ketoconazole (KTZ; 50 mg/kg in corn oil) or troleandomycin (TAO; 100 mg/kg in corn oil) was injected ip into the mice. The doses of the inhibitors have been used in previous studies (Jin *et al.*, 2009; Pellinen *et al.*, 1994). Blood samples were collected 3 h (for assay of the plasma concentration of CBZ and its metabolites) or 24 h (for measurement of the ALT and AST levels) after the last CBZ administration.

Administration of a TLR4 antagonist and an anti-mouse RAGE antibody. Mice were iv treated with eritoran, a TLR4 antagonist, (50 μg/mouse in 0.2 ml sterile saline) or ip treated with an anti-mouse RAGE antibody (100 μg anti-mouse RAGE antibody in 0.5 ml sterile PBS) 6 h after the last CBZ administration using previously described methods (Chavakis *et al.*, 2003; Savov *et al.*, 2005).

Administration of an anti-mouse IL-17 antibody. According to our previous report (Kobayashi *et al.*, 2009), in the neutralization study, mice were ip treated with anti-mouse IL-17 antibody (100 μg anti-mouse IL-17 antibody in 0.5 ml sterile PBS) 6 h after the last CBZ administration. As a control, rat IgG2a was administered (100 μg rat IgG2a in 0.5 ml sterile PBS).

Quantitation of hepatic MPO-positive cells. The infiltration of mononuclear cells was assessed by immunostaining for MPO. A rabbit polyclonal antibody against MPO was used for immunohistochemical staining of the liver as previously described (Kumada *et al.*, 2004). Five visual fields of 400× magnification (0.1 mm^2 each) were randomly selected from each MPO-immunostained specimen, and a picture was taken with a digital camera (D-33E, OLYMPUS, Tokyo). The average number of MPO-positive mononuclear cells from five randomly selected visual fields was compared among the specimens.

Treatment with PGE1. Nine hours after the last CBZ administration, mice were ip treated with PGE_1 (50 μg/mouse, dissolved in 0.5 ml sterile saline). As a control, the vehicle was administered.

Statistical analysis. The data are shown as the means ± SEM. Statistical analyses between multiple groups were performed using one-way ANOVA with Dunnett's *post hoc* test for significance between individual groups. Comparisons between two groups were carried out using two-tailed Student's *t*-tests. A value of $p < 0.05$ was considered statistically significant.

RESULTS

Evaluation of CBZ-Induced Liver Injury in BALB/c Mice

CBZ is known to cause hepatotoxicity with inflammation in only a small number of patients. To provide an experimental platform for mechanistic studies of hepatotoxicity, we sought to develop an animal model of CBZ-induced liver injury in mice. Male BALB/c mice were orally administered CBZ at a dose of 400 mg/kg for 5 days. The plasma ALT and AST levels were unaffected by CBZ administration (Fig. 2A). Next, mice were orally administered CBZ at a dose of 800 mg/kg for 5 days, resulting in severe hepatotoxicity in various mice and death in others, presumably due to pharmacological adverse effects during the repeated administration (data not shown). We then successfully established a dosing regimen for hepatic injury without fatality, named "method A," consisting of oral administrations at a dose of 400 mg/kg for 4 days and 800 mg/kg on the 5th day. Mice were administered CBZ by method A, and the plasma ALT and AST levels were significantly increased 24 and 48 h after the last CBZ administration (Fig. 2A). These effects were observed in approximately 75% of the mice. In contrast, 25% of the mice showed no hepatotoxicity, and thus, the SEM values were large. The plasma ALT levels were higher than the AST levels, suggesting that tissue damage induced by CBZ administration might occur predominantly in liver. OXC, which was used as negative control, did not induce hepatotoxicity in the same dosing conditions. During the repeated administration study, the body weight of the mice did not change (data not shown).

We altered the dose of CBZ on the 5th day to 400, 600, or 800 mg/kg. No change in the plasma ALT level was observed in mice administered 400 or 600 mg/kg, whereas the dose of 800 mg/kg induced severe liver injury (Fig. 2B). In the single administration study, the plasma ALT level did not change after any of the experimental doses (Fig. 2C).

In the histological evaluation study, focal necrosis and loss of hepatocytes around the central vein were observed 24 h after the last CBZ administration with method A (Fig. 2D). No histopathological differences were observed among no treatment (NT), the lower dose of CBZ-administered (400 mg/kg for 5 days) and OXC-administered mice (Fig. 2D).

Analysis of the Plasma Concentration of CBZ and Its Metabolites

Changes in the plasma concentration of CBZ and its metabolites, CBZ-10,11-epoxide, trans-10,11-diOH CBZ, 2-OH CBZ, and 3-OH CBZ, were measured in mice with CBZ-induced liver injury. The maximum plasma concentrations of CBZ, CBZ-10,11-epoxide, and trans-10,11-diOH CBZ were observed 1.5 h after the last CBZ administration. In contrast, the time of the highest concentration of 3-OH CBZ was 3 h postadministration (Fig. 3A). The plasma concentration of 2-OH CBZ was too low to detect (data not shown). After the peak times, the plasma concentrations of CBZ and the three metabolites decreased dependently of time (Fig. 3A).

Effects of Cyp3a Inhibitors on CBZ-Induced Liver Injury

CBZ induces many drug metabolism enzymes including CYP3A and CYP2B in the liver (Oscarson *et al.*, 2006).

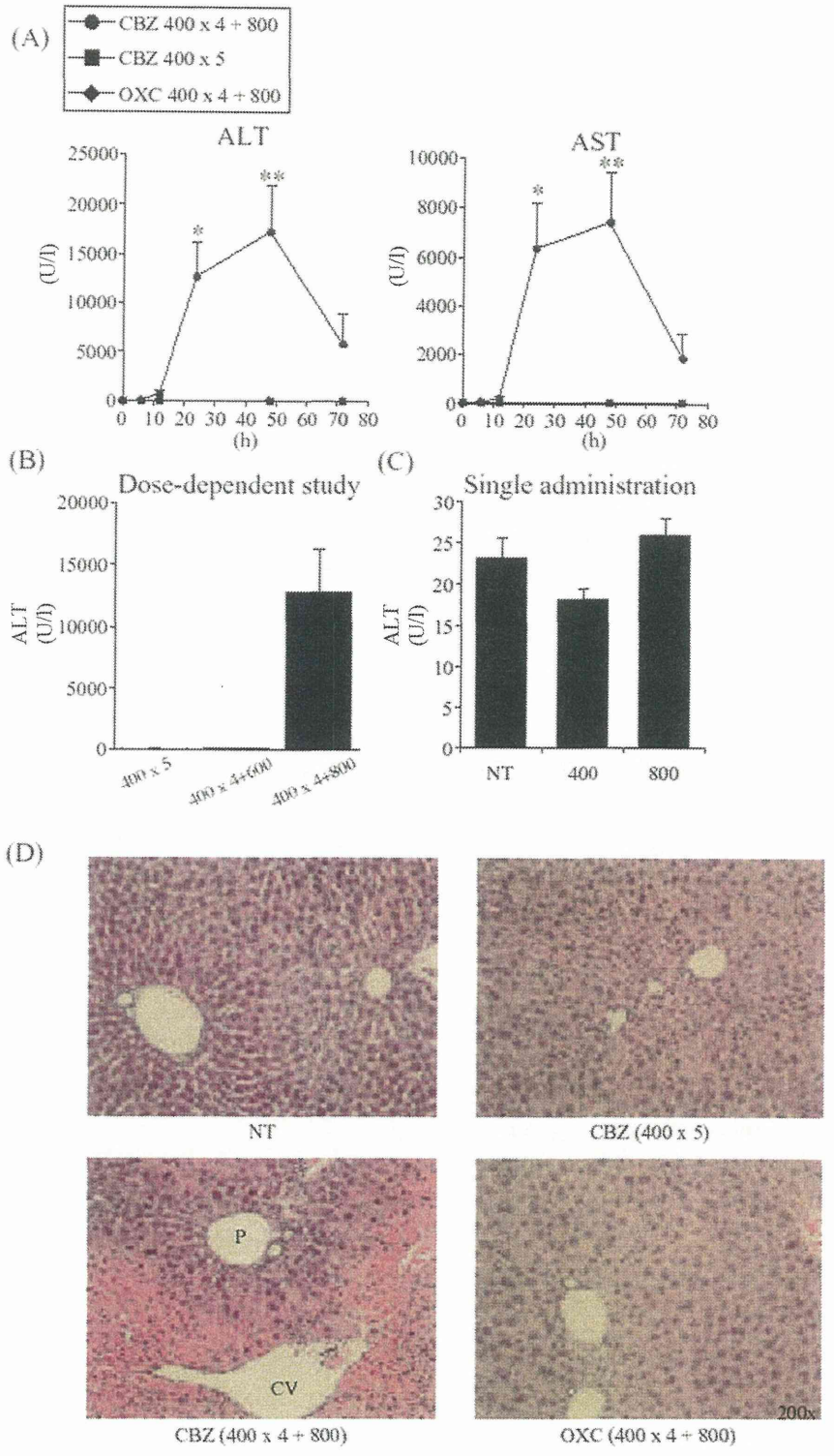

FIG. 2. Time- and dose-dependent changes in plasma ALT and AST levels in CBZ-induced liver injury. Male BALB/c mice were orally administered CBZ by method A (400 mg/kg for 4 days and 800 mg/kg on the 5th day) or 400 mg/kg for 5 days. As the control, mice were administered OXC by method A. At 1.5, 3, 6, 12, 24, 48, and 72 h after the last administration, the blood was collected for assessment of the plasma ALT and AST levels (A). In a dose-dependent study, mice were administered CBZ at a dose of 400 mg/kg for 4 days and 400–800 mg/kg on the 5th day, and blood was collected for assessment of the plasma ALT level 24 h after the last administration (B). In a single administration study, mice were administered CBZ at a dose of 400 mg/kg or 800 mg/kg, and blood was collected 24 h after administration (C). Liver tissue sections were stained with H&E (D). The data are shown as the means ± SEM of the results of the method A group from eight mice and other groups from five mice. Differences compared with the control (0 h) mice were considered significant at $*p < 0.05$ and $**p < 0.01$.

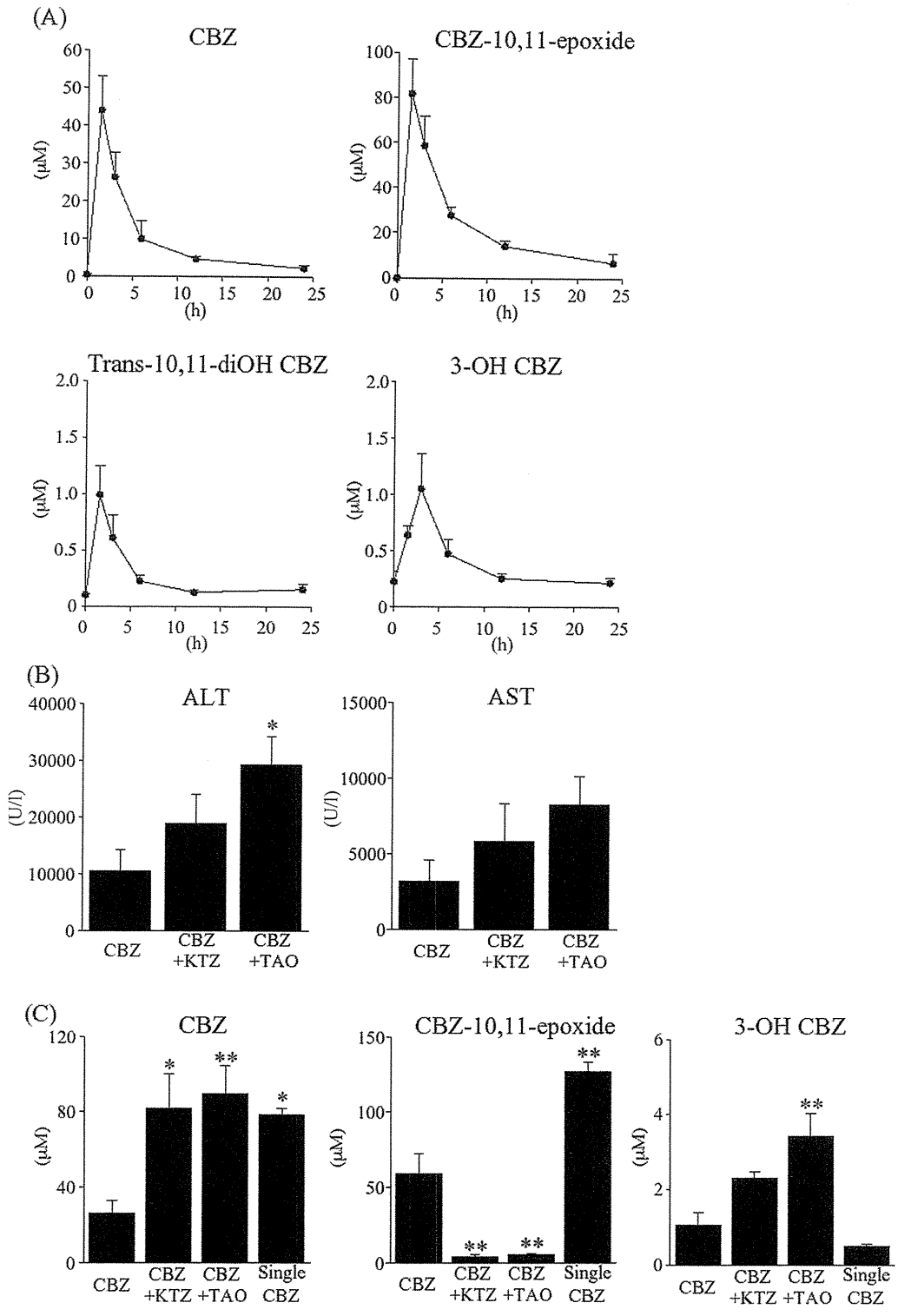

FIG. 3. Changes in the plasma concentration of CBZ and its metabolites and plasma ALT and AST levels in CBZ-induced liver injury. Mice were orally administered CBZ by method A. At 1.5, 3, 6, 12, and 24 h after the last CBZ administration, the blood was collected for assessment of CBZ and its metabolites in plasma (A). The data are shown as the means ± SEM of the results from five mice. The plasma ALT and AST levels and the concentration of CBZ and its metabolites were measured after the administration of Cyp inhibitors in mice with CBZ-induced liver injury (B and C). One hour before the last CBZ administration, KTZ (50 mg/kg in corn oil) or TAO (100 mg/kg in corn oil) was ip administered. Blood samples were collected 3 h (for assay of the plasma concentration of CBZ and its metabolites) or 24 h (for measurement of the ALT and AST levels) after the last CBZ administration. The data are shown as the means ± SEM of the results from five mice. Differences compared with the CBZ-alone-administered mice were considered significant at $^{*}p < 0.05$ and $^{**}p < 0.01$.

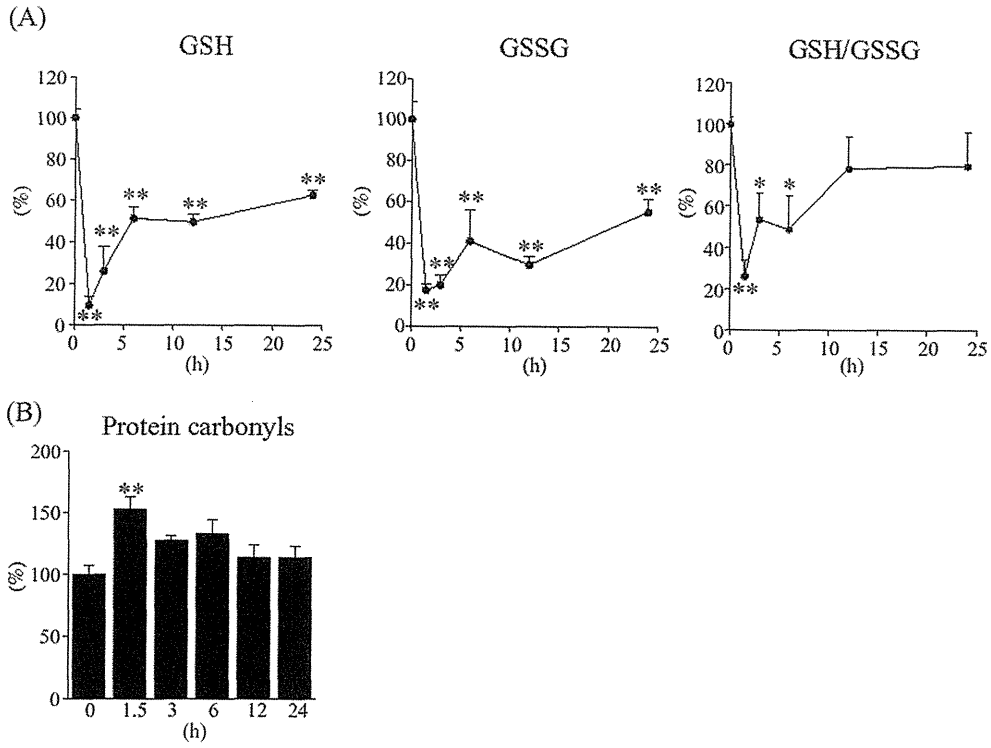

FIG. 4. Time-dependent changes in hepatic GSH, GSSG, and oxidative stress marker levels. Mice were orally administered CBZ by method A. At 1.5, 3, 6, 12, and 24 h after the last CBZ administration, the livers and the plasma were collected for assessment of the hepatic GSH and GSSG levels and GSH/GSSG ratio (A) and the content of plasma protein carbonyls (B). The data are shown as the means ± SEM of the results from five mice. Differences compared with the 0 h mice were considered significant at $*p < 0.05$ and $**p < 0.01$.

CYP3A metabolizes CBZ into CBZ-10,11-epoxide, 3-OH CBZ, and reactive metabolites *in vitro* (Lu and Uetrecht, 2008; Pirmohamed *et al.*, 1992b), leading to the hypothesis that CYP3A may be involved in CBZ-induced toxicity. To investigate whether Cyp3a is involved in CBZ-induced liver injury *in vivo*, mice were treated with the Cyp3a inhibitors KTZ or TAO. Surprisingly, the plasma ALT levels significantly increased after TAO treatment and exhibited an increasing trend after KTZ treatment in CBZ-administered mice. The plasma AST levels also exhibited an increasing trend after KTZ or TAO treatment in CBZ-administered mice (Fig. 3B). Single administration of KTZ (50 mg/kg, ip) or TAO (100 mg/kg, ip) caused no increase in the plasma ALT level 1 h (24.2 ± 6.3 U/l or 27.3 ± 3.7 U/l, respectively) and 25 h (19.8 ± 6.6 U/l or 19.3 ± 5.4 U/l, respectively) after the administration, suggesting KTZ or TAO did not induce hepatotoxicity in the present dosing condition.

The plasma concentrations of CBZ, CBZ-10,11-epoxide, and 3-OH CBZ 3 h after the coadministration of CBZ and KTZ or TAO are shown in Figure 3C. Mice that were administered a single dose of CBZ (800 mg/kg), which caused no hepatotoxicity (Fig. 2C), were used as negative controls. KTZ or TAO treatment significantly increased the plasma concentration of CBZ and significantly decreased the concentration of CBZ-10,11-epoxide, whereas the plasma concentrations of both compounds were significantly increased in mice administered a single dose of CBZ. KTZ exhibited an increasing trend and TAO significantly increased 3-OH CBZ, which exhibited a decreasing trend in mice administered a single dose of CBZ. These data suggest that Cyp3a might be involved in detoxification in CBZ-induced liver injury.

To confirm the Cyp induction by CBZ or OXC with the administration by method A, we measured Cyp3a activity in the microsomes of mice using the metabolism of midazolam as an indicator. The Cyp3a activities were significantly higher in both CBZ- and OXC-administered mice compared with NT mice (Supplementary fig. 1). Because Cyp3a activity was significantly increased in OXC-administered mice, mice were coadministered OXC and TAO, but plasma ALT or AST level was not changed (data not shown).

Changes in GSH Levels and the GSH/Glutathione Disulfide Ratio in the Liver

To investigate whether GSH is involved in detoxification *in vivo* in mice, time-dependent changes in GSH and glutathione disulfide (GSSG) levels in the liver were measured. The GSH level was the lowest 1.5 h after the last CBZ administration and was significantly decreased at 1.5, 3, 6, 12, and 24 h compared with mice at 0 h (time for the final administration of CBZ). GSSG level exhibited a similar profile (Fig. 4A).

We measured the GSH/GSSG ratio, a biomarker of oxidative stress (Fig. 4A). The ratio of GSH/GSSG was significantly

decreased 1.5, 3, and 6 h after the last CBZ administration. In addition, the level of protein carbonyls, which is also a marker of oxidative stress, was significantly increased 1.5 h after the last CBZ administration (Fig. 4B). These results suggested that GSH played a protective role, and oxidative stress is involved in an early stage of CBZ-induced liver injury.

The Expressions of Danger Signals and Their Receptors

It has been reported that ROS elevated the expression levels of danger signals, such as S100A8, S100A9, and HMGB1 (Yao and Brownlee, 2010). To investigate whether danger signals are involved in the onset of inflammation, time-dependent changes in the mRNA expression levels of S100A8, S100A9, HMGB1, TLR2, TLR4, TLR9, and RAGE were measured (Fig. 5A). The mRNA expression levels of S100A8 and S100A9 were time-dependently increased and significantly increased 24 h after the last CBZ administration. The expression of TLR4 was significantly increased at 6 h, and the expression level of RAGE was significantly increased at 12 h postadministration; however, the expression levels of HMGB1, TLR2, and TLR9 were not altered. In OXC-administered mice, the mRNA expression levels of danger signal–related genes were not changed compared with the NT control. It is known that HMGB1 is actively secreted from activated immune cells and is also passively released from necrotic cells (Wang *et al.*, 2004). Thus, the release of HMGB1 is not correlated with the increased expression of hepatic HMGB1 mRNA. The plasma concentration of HMGB1 protein was measured using ELISA, and it was significantly increased at 24 h (Fig. 5B).

To investigate whether TLR4 and RAGE signaling were involved in CBZ-induced liver injury, eritoran, a TLR4 antagonist, or a monoclonal anti-RAGE antibody was administered to the mice. Eritoran or anti-RAGE antibody treatment significantly suppressed the plasma ALT and AST levels (Fig. 5C). These results suggested that TLR4 and RAGE activation might be involved in CBZ-induced liver injury.

The Involvement of Cytokines and Chemokines

To investigate the involvement of inflammatory factors in CBZ-induced liver injury, time-dependent changes in the mRNA expression levels of transcriptional factors, cytokines, and chemokines were measured (Fig. 6A). The expression level of ROR-γt was significantly increased 12 h after the last CBZ administration compared with that of NT mice. T-bet was significantly decreased, and GATA-3 was not altered. The expression levels of IL-6, IL-23 p19, FasL, and macrophage inflammatory protein-2 (MIP-2) were significantly increased compared with those of NT mice, whereas IL-12 p35 and IFN-γ were significantly decreased (Fig. 6A). The expression level of IL-17 mRNA was too low to detect (data not shown). In OXC-administered mice, the mRNA expression levels of cytokines and chemokines were not changed compared with the levels in the NT controls.

The plasma concentrations of IL-17 and IL-23 protein measured by ELISA were significantly increased 24 h after the last CBZ administration (Fig. 6B). The plasma concentration of IFN-γ protein could not be detected at any of the tested time points (data not shown).

To investigate whether IL-17 was involved in CBZ-induced liver injury, we conducted a neutralization study. A monoclonal anti-mouse IL-17 antibody was ip administered 9 h after the last CBZ administration, resulting in significantly reduced plasma ALT and AST levels 24 h after the last CBZ administration (Fig. 6C). These effects were not observed after the administration of an IgG control antibody. In the histopathological evaluation study, anti-mouse IL-17 antibody treatment significantly decreased the number of MPO-positive cells (Fig. 6D). Representative photographs of anti-MPO staining are shown in Supplementary figure 2.

Effects of PGE_1 Treatment

PGEs are known to protect against drug-induced and immune-mediated liver injury by downregulating the production of inflammatory cytokines. PGE_1 inhibited the function of neutrophils (Talpain *et al.*, 1995) and the production of IL-17 (Kobayashi *et al.*, 2009). It was reported that IL-6 and IL-23 induced IL-17 production (Langrish *et al.*, 2005). On the basis of these studies, we hypothesized that PGE_1 might decrease the production of IL-6 and IL-23 in the present study. PGE_1 conjugated by α-cyclodextrin was ip injected into mice 9 h after the last CBZ administration according to the method reported previously (Kobayashi *et al.*, 2009). The plasma ALT and AST levels were significantly decreased by PGE_1 treatment in CBZ-administered mice compared with CBZ alone-administered mice (Fig. 7A). PGE_1 administration significantly suppressed the hepatic mRNA expression of IL-6, IL-23p19, and MIP-2 (Fig. 7B). The plasma concentrations of IL-17 and IL-23 proteins were also decreased (Fig. 7C).

DISCUSSION

Advances in the understanding of the mechanisms of drug-induced liver injury have been hampered by the lack of proper animal models. Mouse models of APAP-induced liver injury are the widespread model, but this model alone cannot encompass the entire spectrum of the clinical and mechanistic features of drug-induced liver injury in patients. In the present study, we developed a mouse model of CBZ-induced liver injury. This model provided novel mechanistic information, including aspects of drug metabolism and inflammation in the pathogenesis of CBZ-induced liver injury.

Subacute toxicity study demonstrated that no evidence of hepatotoxicity was observed after repeated administrations of CBZ (200 mg/kg, orally) once daily for 24 weeks to mice (Novartis Pharma Co., 2011). After investigating many different dosing conditions, we found that CBZ at a dose of 400 mg/kg for 4 days and 800 mg/kg on the 5th day (method A) induced prominent hepatotoxicity, but 400 mg/kg for 5 days did not (Fig. 2A). The maximum plasma concentration of CBZ

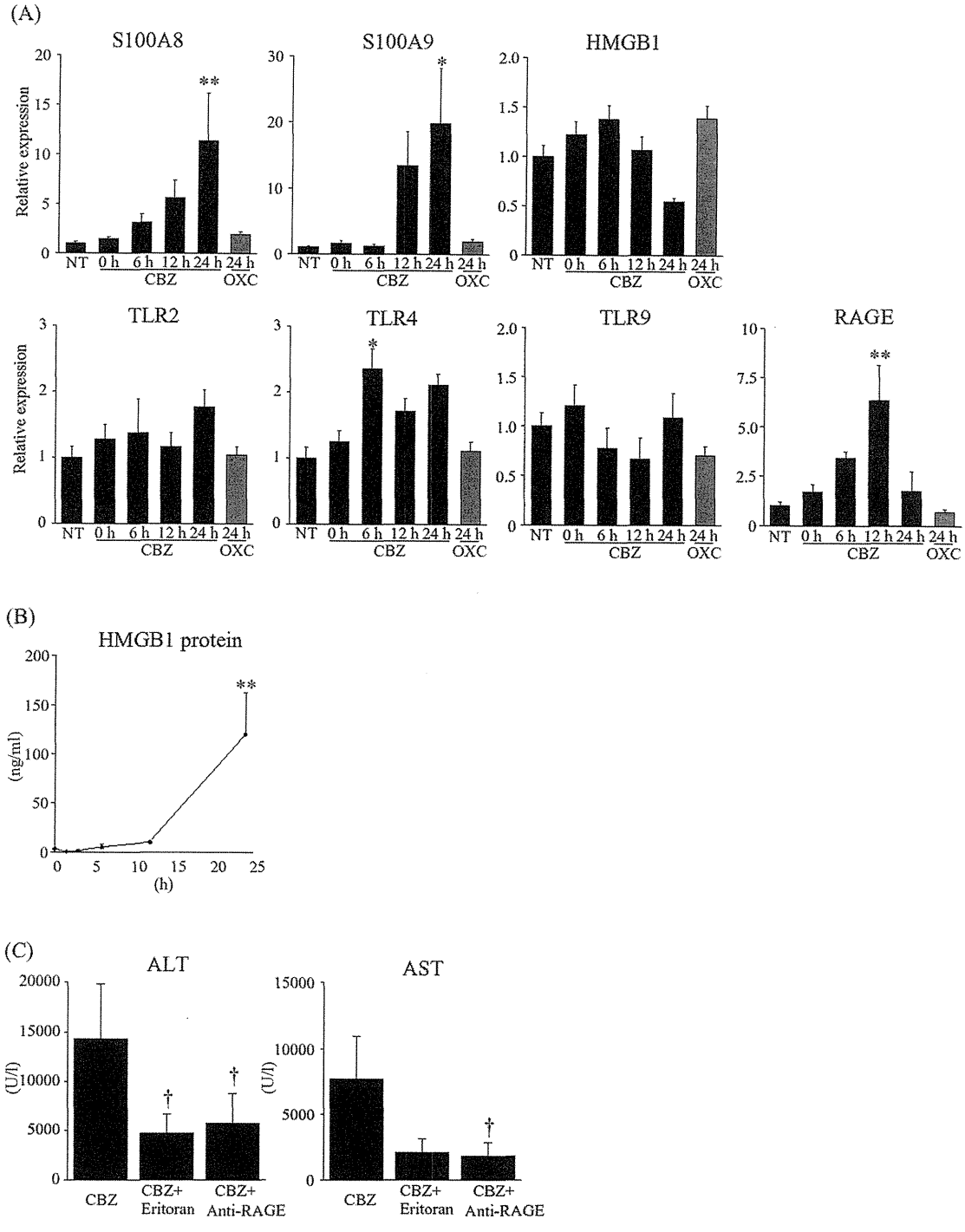

FIG. 5. Time-dependent changes in the mRNA expression levels of danger signal–related genes in the liver of CBZ-administered mice (A) and the plasma HMGB1 protein levels in CBZ-administered mice (B). Mice were orally administered CBZ by method A, and the livers and plasma were collected 0, 6, 12, and 24 h after the last CBZ administration for assessment of the expression levels of the hepatic mRNA or the plasma protein levels. As the control, mice were orally administered OXC by the same method A, and the livers and plasma were collected 24 h after the last OXC administration. The expression of hepatic mRNA was normalized to that of β-actin. The effects of the administration of eritoran, a TLR4 antagonist, or anti-RAGE-monoclonal antibody on CBZ-induced liver injury (C). Mice were iv administered eritoran (50 μg/mouse in 0.1 ml sterile saline) or ip anti-mouse RAGE antibody (100 μg anti-RAGE antibody in 0.5 ml sterile PBS) 6 h after the last CBZ administration. Blood samples were collected 24 h after the last CBZ administration. The data are shown as the means ± SEM of the results of the time-dependent study from five mice, the method A group from eight mice, and the other groups from five mice. Differences compared with the 0 h mice were considered significant at $*p < 0.05$ and $**p < 0.01$, and differences compared with the CBZ-alone-administered mice were considered significant at $\dagger p < 0.05$.

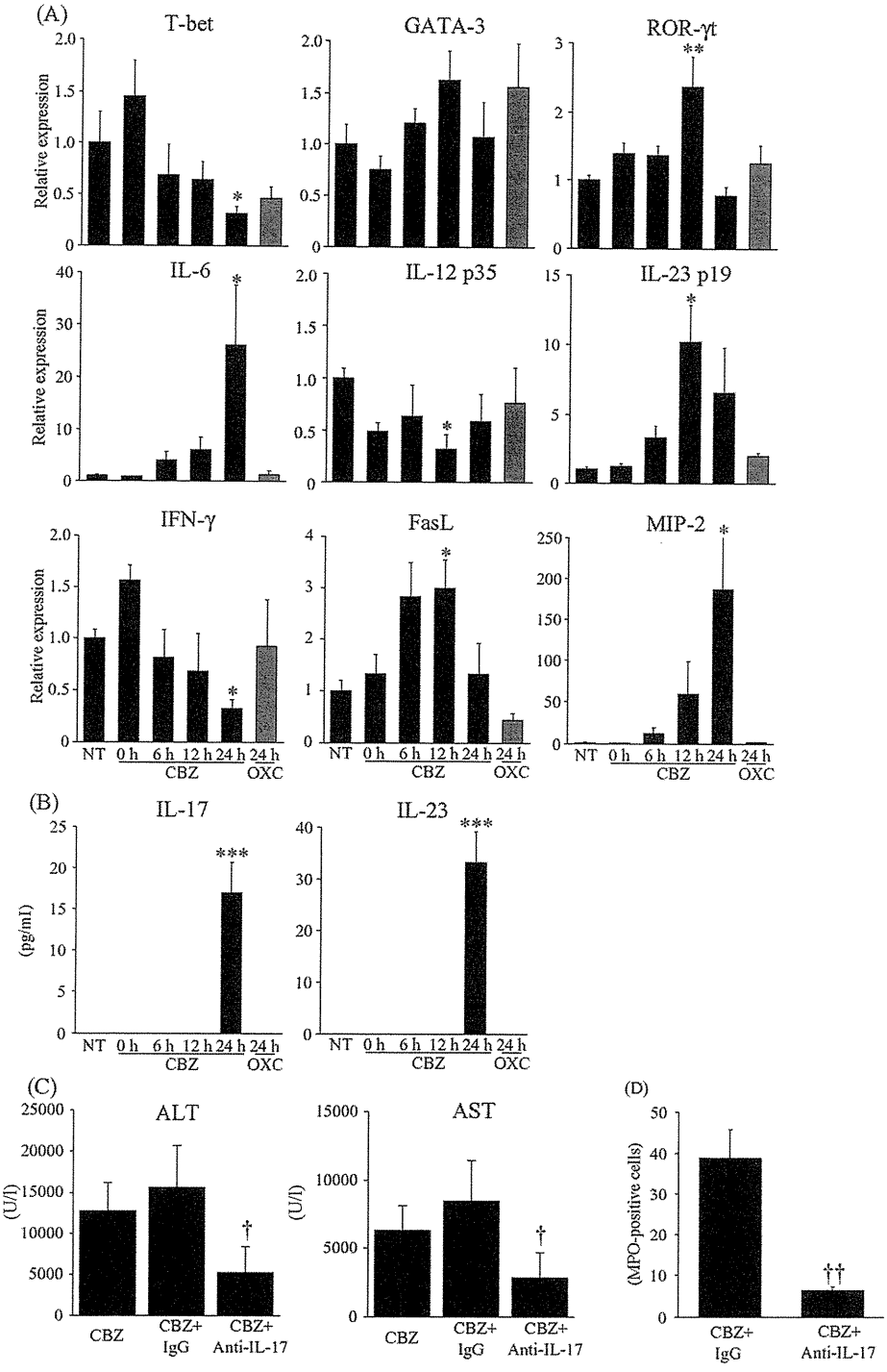

FIG. 6. Time-dependent changes in the hepatic mRNA expression levels and plasma protein levels of proinflammatory cytokines and chemokines in CBZ-induced liver injury (A and B). Mice were orally administered CBZ by method A, and the livers and the plasma were collected 0, 6, 12, and 24 h after the last CBZ administration for assessment of the expression levels of the hepatic mRNA by real-time RT-PCR or the plasma protein levels by ELISA. Mice were orally administered OXC by the same method A, and the livers and plasma were collected 24 h after the last administration. The expression of hepatic mRNA was normalized to that of β-actin. The data are shown as the means ± SEM of the results from five mice. Differences compared with the NT mice were considered significant at $^{*}p < 0.05$, $^{**}p < 0.01$, and $^{***}p < 0.001$. The neutralization study of IL-17 in CBZ-induced liver injury (C). Mice were ip administered an anti-mouse IL-17 antibody (100 μg anti-mouse IL-17 antibody in 0.5 ml sterile PBS) 6 h after the last CBZ administration. As a control, rat IgG2a was administered (100 μg rat IgG2a in 0.5 ml sterile PBS). The number of MPO-positive cells in CBZ-alone-administered mice or CBZ and anti-IL-17-administered mice (D). The infiltration of mononuclear cells was assessed by immunostaining for MPO. The data are shown as the means ± SEM of the results of the method A group from eight mice and the other group from six mice. Differences compared with the CBZ- and IgG-administered mice were considered significant at $\dagger p < 0.05$ and $\dagger\dagger p < 0.01$.